Cancer Cell

Article

Dynamics of molecular heterogeneity in high-risk luminal breast cancer—From intrinsic to adaptive subtyping

Graphical abstract

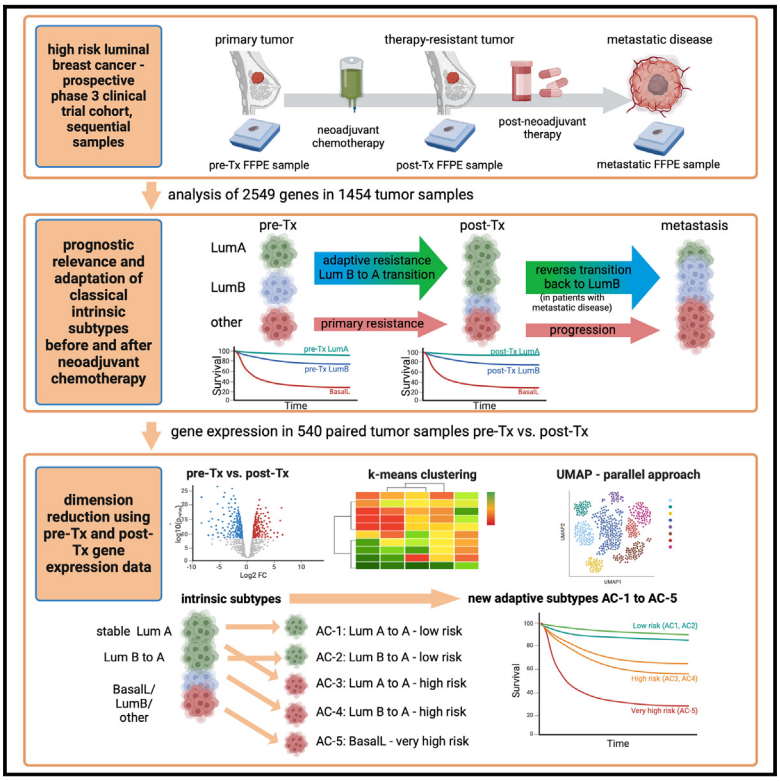

Highlights

- Classical intrinsic subtypes change during neoadjuvant therapy from LumB to LumA
- A reverse-transition back to LumB is observed in metastatic disease
- Improved dimension reduction by comparison of pre- and post-therapeutic samples
- Identification of adaptive prognostic subsets in high-risk luminal breast cancer

Authors

Carsten Denkert, Sivaramakrishna Rachakonda, Thomas Karn, ..., Johannes Holtschmidt, Valentina Nekljudova, Sibylle Loibl

Correspondence

carsten.denkert@uni-marburg.de (C.D.), sibylle.loibl@gbg.de (S.L.)

In brief

Denkert et al. evaluate adaptation of luminal high-risk breast cancer to neoadjuvant therapy in longitudinal biopsies from Penelope-B trial and identify five adaptive subtypes (AC1-5) by comparing pre- and post-therapeutic paired tumor samples, supporting an extended molecular classification of breast cancer patients for the identification of high-risk populations.

Denkert et al., 2025, Cancer Cell *43*, 232–247
February 10, 2025
https://doi.org/10.1016/j.ccell.2025.01.002

CellPress

CellPress
OPEN ACCESS

Cancer Cell

Article

Dynamics of molecular heterogeneity in high-risk luminal breast cancer—From intrinsic to adaptive subtyping

Carsten Denkert,[1,*] Sivaramakrishna Rachakonda,[2] Thomas Karn,[3] Karsten Weber,[2] Miguel Martin,[4,5] Frederik Marmé,[6] Michael Untch,[7,8] Hervé Bonnefoi,[9] Sung-Bae Kim,[10] Sabine Seiler,[2] Harry D. Bear,[11] Agnieszka K. Witkiewicz,[12] Seock-Ah Im,[13] Angela DeMichele,[14] Anika Pehl,[1] Laura van't Veer,[15] Nicole McCarthy,[16] Thorsten Stiewe,[17]

(Author list continued on next page)

[1]Institute of Pathology, Philipps-University Marburg and University Hospital Marburg, Marburg, Germany
[2]German Breast Group, Neu-Isenburg, Germany
[3]Department of Gynecology and Obstetrics, Goethe-University, Frankfurt, Germany
[4]Instituto de Investigacion Sanitaria Gregorio Marañon, CIBERONC, Universidad Complutense, Madrid, Spain
[5]Spanish Breast Cancer Group, GEICAM, Madrid, Spain
[6]Medical Faculty Mannheim, Heidelberg University, University Hospital Mannheim, Mannheim, Germany
[7]Helios Kliniken Berlin-Buch, Berlin, Germany
[8]AGO-B Study Group, Erlangen, Germany
[9]Institut Bergonié and Université de Bordeaux UFR Collège Sciences de la Santé, INSERM U1312, Bordeaux, France
[10]Asan Medical Center, University of Ulsan College of Medicine, Seoul, Republic of Korea

(Affiliations continued on next page)

SUMMARY

We evaluate therapy-induced molecular heterogeneity in longitudinal samples from high-risk, hormone-receptor positive/HER2-negative breast cancer patients with residual tumor after neoadjuvant chemotherapy from the Penelope-B trial (NCT01864746; EudraCT 2013-001040-62). Intrinsic subtypes are prognostic in pre-therapeutic (Tx) samples (n = 629, $p < 0.0001$) and post-Tx residual tumors (n = 782, $p < 0.0001$). After neoadjuvant chemotherapy, a shift of intrinsic subtypes is observed from pre-Tx luminal (Lum) B to post-Tx LumA, with reverse transition back to LumB in metastases. In a combined analysis of 540 paired pre-Tx and post-Tx samples, we identify five adaptive clusters (AC-1–5) based on transcriptomic changes before and after neoadjuvant chemotherapy. These AC-subtypes are prognostic beyond classical intrinsic subtyping, categorizing patients into groups with excellent prognosis (AC-1 and AC-2), poor prognosis (AC-3 and AC-4), and very poor prognosis (AC-5, enriched for basal-like subtype). Our analysis provides a basis for an extended molecular classification of breast cancer patients and improved identification of high-risk patient populations.

INTRODUCTION

Molecular subtyping of tumor biopsies[1,2] revealed that breast cancer constitutes a heterogeneous set of diseases with different biological features, requiring tailored therapeutic strategies.[3] In addition, genomic signatures have been developed to predict the response to neoadjuvant chemotherapy (NACT), with a strong contribution of immune gene expression.[4–6] For luminal breast cancer, clinical strategies[7,8] are based on prognostic assessment of tumor samples before therapy[9–11] to identify those patients who can be treated with endocrine therapy alone, without additional chemotherapy. These approaches have led to considerable advances in the clinical management of breast cancer with therapeutic algorithms in place for the different subtypes. However, molecular changes in the tumor after neoadjuvant therapy as well as tumor heterogeneity[12] constitute a major clinical problem,[13] and the subsequent treatment of therapy-resistant recurrent and metastatic disease remains challenging.

Post-neoadjuvant adaptive treatment has become the standard for therapy-resistant HER2-positive[14] and triple-negative breast cancer,[15] leading to improvement of overall survival. Response-guided therapy based on clinical assessment of early response to NACT leads to improved outcome in hormone-receptor (HR) positive breast cancer.[16] The pathological complete response rate (pCR) of luminal tumors to neoadjuvant chemotherapy is generally lower compared to other subtypes.[17,18] It has recently been shown that in high-risk luminal tumors, addition of immunotherapy to NACT increases the pCR rate,[19,20] and it will be important to define the subgroup of patients who will derive most benefit from this neoadjuvant approach.

CellPress
OPEN ACCESS

Paul Jank,[1] Karen A. Gelmon,[18] José A. García-Sáenz,[19] Christina C. Westhoff,[1] Catherine M. Kelly,[20] Toralf Reimer,[21] Bärbel Felder,[2] Mireia Melé Olivé,[22] Erik S. Knudsen,[12] Nicholas Turner,[23] Federico Rojo,[5,24] Wolfgang D. Schmitt,[25] Peter A. Fasching,[26] Julia Teply-Szymanski,[1] Zhe Zhang,[27] Masakazu Toi,[28,29] Hope S. Rugo,[30] Michael Gnant,[31] Andreas Makris,[32] Johannes Holtschmidt,[2] Valentina Nekljudova,[2] and Sibylle Loibl[2,33,*]

[11]Division of Surgical Oncology, Massey Comprehensive Cancer Center, Virginia Commonwealth University, VCU Health, Richmond, VA, USA
[12]Roswell Park Comprehensive Cancer Center, Buffalo, NY, USA
[13]Seoul National University Hospital, Seoul National University College of Medicine, Seoul, Republic of Korea
[14]Penn Medicine Abramson Cancer Center, Philadelphia, PA, USA
[15]University of California, San Francisco, San Francisco, CA, USA
[16]Breast Cancer Trials Australia and New Zealand and University of Queensland, Queensland, Brisbane, Australia
[17]Genomics Core Facility, Philipps-University Marburg, Marburg, Germany
[18]BC Cancer, Vancouver, BC, Canada
[19]Service de Oncología Médica, Hospital Clínico San Carlos, Madrid, Spain
[20]Mater Private Hospital, Dublin and Cancer Trials Ireland Breast Group, Dublin, Ireland
[21]Department of Obstetrics and Gynecology, University of Rostock, Rostock, Germany
[22]Hospital Universitari Sant Joan de Reus, Tarragona, Spain
[23]Royal Marsden Hospital and Institute of Cancer Research, London, UK
[24]Hospital Universitario Fundación Jiménez Díaz, Madrid, Spain
[25]Charité – Universitätsmedizin Berlin, corporate member of Freie Universität Berlin and Humboldt Universität zu Berlin, Institute of Pathology, Berlin, Germany
[26]University Hospital Erlangen, Department of Gynecology and Obstetrics, Comprehensive Cancer Center Erlangen-EMN, Friedrich-Alexander University Erlangen-Nuremberg, Erlangen, Germany
[27]Pfizer Inc., San Diego, CA, United States of America
[28]Breast Surgery, Graduate School of Medicine, Kyoto University, Kyoto, Japan
[29]Tokyo Metropolitan Cancer and Infectious Disease Center, Komagome Hospital, Tokyo, Japan
[30]University of California San Francisco Comprehensive Cancer Center, San Francisco, CA, USA
[31]Comprehensive Cancer Center, Medical University of Vienna, Vienna, Austria
[32]Mount Vernon Cancer Centre, Northwood, UK
[33]Lead contact
*Correspondence: carsten.denkert@uni-marburg.de (C.D.), sibylle.loibl@gbg.de (S.L.)
https://doi.org/10.1016/j.ccell.2025.01.002

Luminal tumors consist of two different subtypes: luminal A (LumA) tumors have a low proliferation rate and are typically treated with endocrine therapy alone. In contrast, luminal B (LumB) tumors are characterized by increased proliferation and tumor aggressiveness and therapeutic strategies for these tumors often include chemotherapy, followed by endocrine therapy. The definition of LumA and LumB tumors is based on gene expression profiling, including the PAM50[21] approach as well as absolute intrinsic molecular subtyping (AIMS)-based subtyping.[22] In addition, other molecular assays as well as proliferation markers such as Ki67[23] are used. Adaptive changes of Ki67 can be used to decide whether patients should receive endocrine therapy or chemotherapy followed by endocrine therapy.[24,25] Due to the limited availability of paired samples, little is known about the changes of molecular subtypes during and after therapy. Therefore, an improved understanding of molecular adaptation to neoadjuvant chemotherapy could generate new advanced options for classification of tumors and tailored therapeutic strategies.

In this study, we evaluated a large clinical trial cohort of hormone HR-positive, HER2-negative tumors from the post-neoadjuvant trial Penelope-B.[26] The trial cohort was selected for patients with chemotherapy-pretreated high-risk tumors with high clinical risk after neoadjuvant chemotherapy,[27] and all had residual disease after NACT. We hypothesized that neoadjuvant chemotherapy could lead to changes in molecular subtypes and underlying changes in gene expression. Analyzing these alterations may improve our understanding of therapy resistance mechanisms in luminal breast cancer. To achieve this, we focused on longitudinal gene expression changes in samples collected at baseline (pre-Tx), after neoadjuvant chemotherapy (post-Tx) and at relapse in metastatic disease. As a first step, we evaluated changes in molecular subtypes, particularly the molecular transition between LumA and LumB tumors, during therapy and in paired metastatic biopsies. For an advanced classification of these therapy-resistant tumors, we identified genes that significantly differed in paired pre- and post-therapeutic biopsies. Our findings indicate that these genes can be used in the pretherapeutic setting to identify different prognostic groups of clinically chemotherapy resistant breast cancer.

RESULTS

Study cohort and baseline clinical data

All 1,250 patients randomized (Figure 1A) had HR-positive, HER2-negative tumors with invasive residual disease after NACT and a CPS-EG (clinical stage, pathologic stage, ER-status and tumor grade) score[27–29] of ≥ 3 or of ≥ 2 with positive lymph nodes. Gene expression data were obtained from 629 pre-therapeutic and 782 post-therapeutic samples (Figure 1B). For 540 patients paired data from both time points were available. In addition, samples from 43 distant relapses were analyzed; in 29 patients, data from three time points were available. The Kaplan-Meier plot (Figure 1C) shows that Penelope-B is a high-risk cohort with no difference between the two post-NACT therapy arms, as previously reported.[26] The baseline characteristics are shown in Table S1.

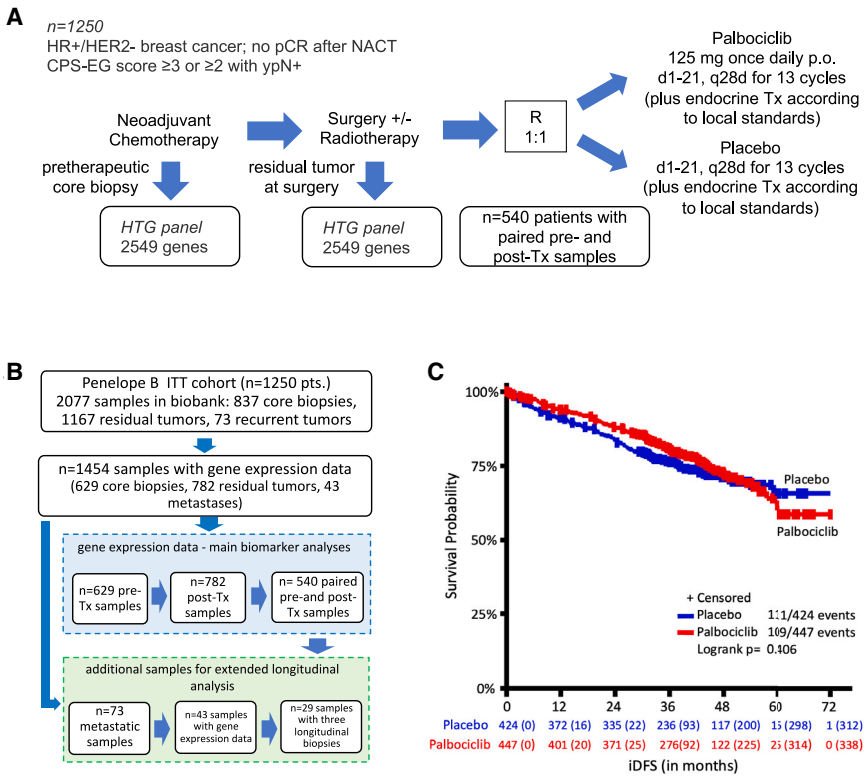

Figure 1. The Penelope-B clinical trial cohort was used for evaluation of longitudinal biomarkers

(A) Study outline. Inclusion parameters were patients with hormone-receptor positive, HER2-negative early breast cancer and no pCR after neoadjuvant chemotherapy and a CPS-EG score of either ≥ 3 or of ≥ 2 with ypN+. Based on these inclusion criteria, 1,250 patients were randomized to post-neoadjuvant palbociclib vs. placebo.

(B) Consort statement for main biomarker cohorts. Gene expression analysis was performed in 629 pre-Tx core biopsies and 782 post-Tx samples. For 540 patients, paired pre- and post-Tx gene expression data were available. These three cohorts of 629, 782, and 540 patients were used for the main analyses. In addition, 43 samples from metastatic tumors were analyzed. For 29 patients, longitudinal samples pre-Tx, post-Tx, and metastatic disease were available.

(C) Kaplan-Meier analysis of all patients with available biomaterial, indicating that the inclusion criteria for the Penelope-B trial define a high-risk luminal breast cancer cohort. In the biomarker cohort, there is no significant therapy effect of post-NACT palbociclib vs. placebo, similar to the complete study cohort. See also Table S1.

Changes in molecular subtypes of breast cancer in pre- and post-Tx samples

We evaluated the prevalence and prognostic role of AIMS subtypes in 629 tumor samples before chemotherapy. Figure 2A shows the distribution of subtypes in pre-Tx biopsies, with 324 (51.51%) LumA, 270 (42.93%) LumB, 22 (3.50%) HER2-enriched (HER2E), 11 (1.75%) basal-like (BasalL), and 2 (0.32%) normal-like (NormL) tumors. As expected, these subtypes were highly prognostic (Figure 2B, $p < 0.0001$, log rank test).

As shown in Figure 2C, the distribution of the AIMS subtypes differed significantly in 782 post-Tx samples, with 76.6% LumA and only 8.2% LumB tumors. The NormL group was increased to 10%, while still only few tumors were HER2E (3.3%) or BasalL (1.9%).

In Kaplan-Meier analysis of post-Tx AIMS subtypes (Figure 2D), we observed a strong prognostic effect ($n = 782$) with a better prognosis for NormL and LumA, a worse prognosis for LumB tumors, and a very poor prognosis for BasalL and HER2E tumors. Figure S1A shows the tumor content in post-NACT samples, which was lowest in the NormL subtype. A paired analysis of 540 tumors with pre- and post-NACT samples shows the transition from LumB to LumA as main alteration during NACT (Figure 2E). Patients whose tumors changed from LumB to A had a similar prognosis for the first 24 months as consistently LumA tumors (Figure 2F), with a separation of the curves after 24 months. In a separate analysis of all 232 pre-Tx LumB tumors, those tumors with a persistent LumB phenotype had a poor prognosis compared to tumors that changed to LumA during NACT (Figure S1B).

Reverse subtype transition in metastatic disease

We also analyzed 43 metastatic samples, which were mainly LumB (24 of 43, 55.81%). The second largest group were HER2E tumors (11 of 43, 25.58%) and only 9.30% were LumA (Figure 2G). For 29 patients, we evaluated the temporal evolution of molecular subtypes in three longitudinal samples before and after NACT and in metastatic disease. We found that the AIMS subtype transition from LumB to LumA during the NACT was reversed back to LumB in patients who developed metastatic disease (Figure 2H).

Adaptive profiling of paired tumor samples

As a next step, we analyzed alterations in gene expression during NACT. We identified 335 differentially expressed genes (DEG) comparing pre-Tx and post-Tx samples (false discovery rate [FDR] < 0.05; logFC ± 0.58, Figures 3A and S2). Hierarchical clustering of all 1,080 samples (540 pre-Tx and 540 post-Tx) based on expression of these 335 DEGs led to a clear separation of pre- and post-Tx samples and identified additional clusters of tumors (Figure 3B). Within the pre-Tx samples, four main clusters (“adaptive clusters” AC-1 to AC-4) and a small group of BasalL/HER2E (AC-5) tumors could be separated. Interestingly, Kaplan-Meier analysis showed major differences in prognosis for the five AC-groups ($p = 0.0001$, Figure 3C), indicating that DEGs before and after therapy could be the basis for new prognostic groups of breast cancer. Patients in two large groups of tumors (AC-1 and AC-2) displayed an excellent prognosis, while those in cluster AC-3 and AC-4 had a poor prognosis. In addition, the small group of BasalL/HER2E tumors (AC-5) was characterized by a very

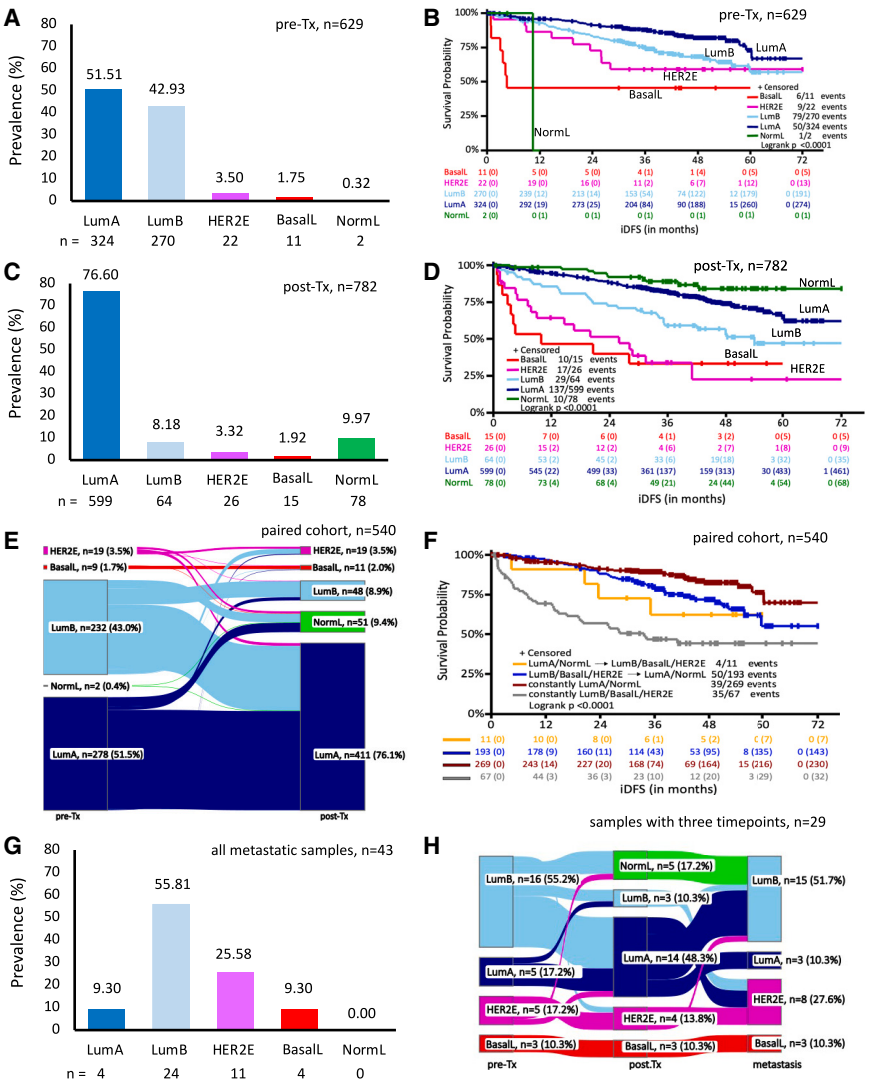

Figure 2. Molecular breast cancer subtypes are changed during neoadjuvant therapy and in metastatic disease

(A) Prevalence of AIMS subtypes in pretherapeutic core biopsies (pre-Tx, $n = 629$).

(B) Prognostic relevance of AIMS subtypes in pre-Tx core biopsies ($p < 0.0001$, log rank test).

(C) Distribution of AIMS subtypes in post-therapeutic residual tumors (post-Tx, $n = 782$).

(D) Prognostic relevance of AIMS subtypes after neoadjuvant chemotherapy ($p < 0.0001$).

(E) Sankey diagram. Paired analysis of 540 tumors before and after therapy showing the transition from LumB to LumA as the main alteration during neoadjuvant therapy.

(F) Survival analysis comparing tumors with subtype transition and tumors with constant AIMS subtypes.

(G) Analysis of AIMS subtypes in metastatic tumors. Also see Figures S1 and S6.

(H) Sankey diagram of longitudinal AIMS-subtypes in $n = 29$ patients with no response to chemotherapy and three longitudinal tumor samples indicating a transition from LumB to LumA in the chemotherapy phase that is reversed in metastatic disease.

poor prognosis. The patient clusters AC-6 to AC-9 in the post-Tx samples were not prognostic (Figure 3D). A standardized centroid-based classifier for the AC-1 to AC-5 subgroups resulted in a similar prognostic performance in the cohort of 540 pre-Tx samples alone, without integration of paired post-Tx samples (Figure S2).

Evaluation of prognostic genes and gene sets in pre-Tx and post-Tx samples

We evaluated the prognostic role of the 335 DEGs in pre-Tx and post-Tx samples. The results are shown in Figures 4A–4D as a scatterplot based on the prognostic values of all individual genes that are differentially expressed between pre-Tx and post-Tx and are also prognostic in either the pre-Tx or the post-Tx cohort. The individual genes are distributed into four quadrants based on their concordant or discordant prognostic impact in the pre-Tx and the post-Tx cohort. Figure 4E shows the expression of selected genes in pre-Tx and post-Tx samples; the prognostic impact of these genes pre-Tx and post-Tx is shown in Figure 4F. Interestingly, the genes *OGG1*, *DNAJC14*, *POLR2D*, *LIG4*, *NME1*, and *NTHL1* show a very strong positive prognostic impact in pre-Tx biopsies, but this positive prognostic effect is not observed in post-Tx samples. In contrast, the genes *TEK*, *TNFRSF1B*, *TIPARP*, and *VCAM1* are significant for good prognosis in the resection specimen and for poor prognosis in the biopsy.

Gene set enrichment analysis (GSEA) revealed differences in molecular pathways regulating cellular processes such as proliferation, DNA repair and EGF/PDGF signaling before and after NACT (Figure S3A). In addition, we performed a GSEA analysis for prognostic gene sets independently in the pre-Tx and the post-Tx samples (Figure S3B). Immune gene sets had a positive impact on prognosis both in pre-Tx and post-Tx samples, and proliferation-related gene sets had a negative impact on prognosis in pre-Tx and post-Tx tumors.

Interestingly, some gene sets displayed an opposite prognostic value in the pre-Tx and post-Tx cohorts (Figure S3B, lower right and upper left quadrant). For example, DNA-repair showed a positive prognostic association in pre-Tx, but a negative association in post-Tx samples and IL6-Jak-Stat-signaling showed a negative prognostic association in pre-Tx but a positive association in post-Tx biopsies.

The contribution of different gene clusters to the five AC-subtypes is shown in Figure S4. Gene cluster 1 is the most important gene cluster for distinction between the good prognosis groups AC-1 and AC-2 vs. the poor prognosis groups AC-3 and AC-4. This gene cluster contains genes involved in interferon (IFN)-response, estrogen-signaling, and DNA repair/stress response. Gene cluster 2 contains proliferation markers and distinguishes

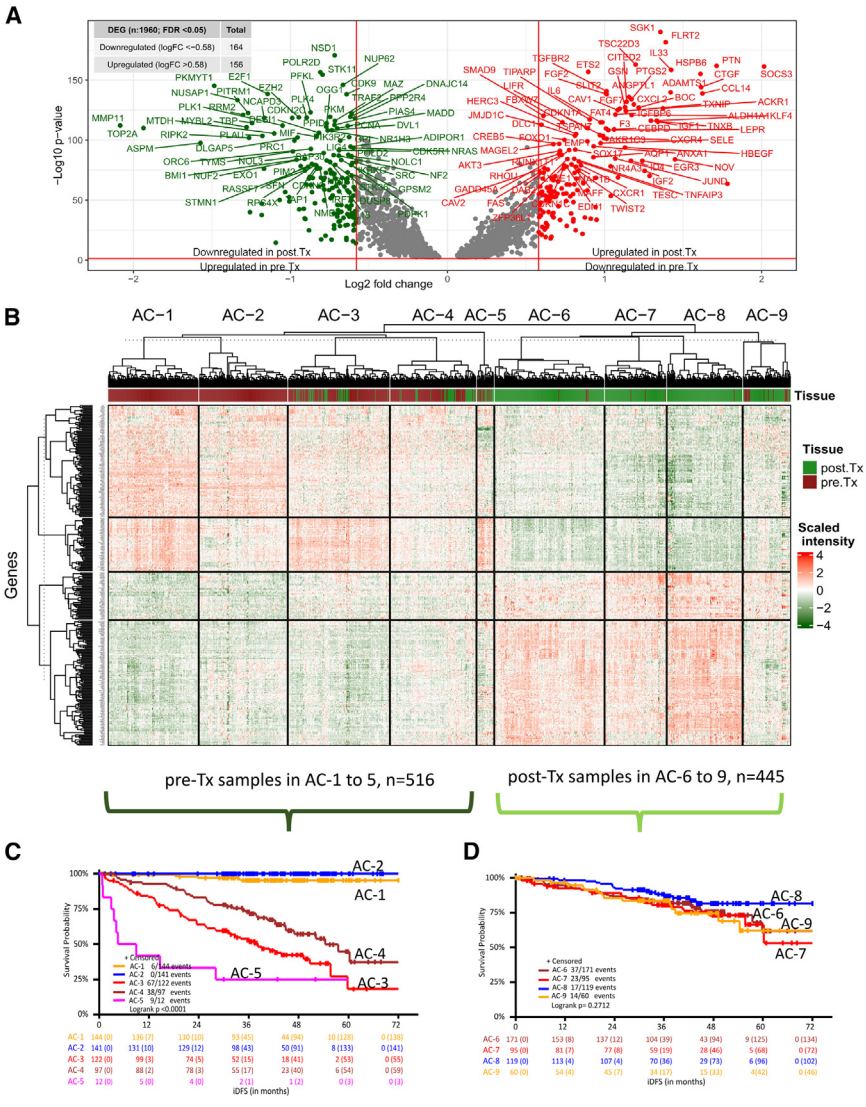

Figure 3. Analysis of molecular alterations induced by neoadjuvant chemotherapy leads to identification of adaptive clusters as new prognostic subgroups of breast cancer

(A) Comparison of pre-Tx and post-Tx tumors samples with 320 of 335 differentially expressed genes shown. 15 genes known to be highly inducible by preanalytical factors in surgical samples are removed from this figure, they are included in Figure S2.

(B) Heatmap containing 1,080 tumor samples (540 pre-Tx and 540 post-Tx) as well as 335 differentially expressed genes. Pre-Tx samples are divided into 5 distinct groups (adaptive clusters AC-1 to AC-5), post-Tx samples are divided into four different clusters. Genes are divided into four main gene clusters, reflecting the differences between pre- and post NACT samples as well as between different AC sample clusters.

(C) Kaplan-Meier analysis of the five different adaptive clusters AC-1 to AC-5 in 516 pre-Tx tumors (log rank p value < 0.0001). Pre-Tx tumors that cluster into AC-6 to AC-9 (n = 24) are not included; a complete clustering of all 540 pre-Tx tumors based on centroids is shown in Figure S2.

(D) Kaplan-Meier analysis of the four different adaptive clusters AC-6 to AC-9 in 445 post-Tx tumors (log rank p value 0.27, not significant). Post-Tx tumors that cluster into AC-1-5 (n = 90) are not included. Also see Figures S2, S6 and Video S1.

between LumA and LumB tumors. Gene clusters 3 and 4 contain genes that are typical for stromal tissue, normal breast tissue, and immune cells, these clusters show mainly differences between pre-Tx and post-Tx samples. For a more extensive analysis of the four main gene clusters, we performed a parallel evaluation of the genes included in these clusters in the TCGA (The Cancer Genome Atlas) cohort (Figure S5), showing the contribution of stromal genes typical for normal breast tissue to gene clusters 3 and 4.

Contribution of intrinsic subtypes to the adaptive subtypes

As a next step, we combined information about pre-Tx and post-Tx AIMS groups with the adaptive clustering. There was a defined pattern of pre-Tx AIMS subtypes in the different AC-groups (Figures 5A–5F): AC-1 consisted mainly of LumB-to-A tumors that had a LumB phenotype before therapy and switched to LumA in residual tumors (Figures 5A and 5B). This pattern was also observed in the AC-3 group (Figures 5A and 5D)—with the important difference that AC-1 had an excellent prognosis and AC-3 had a poor prognosis (as shown in Figure 3C). Similarly, AC-2 consisted of LumA-to-A tumors (pre-Tx LumA tumors that remained LumA in residual tumors, Figures 5A and 5C), and was very similar to AC-4 (Figures 5A and 5E), but also with a highly significant difference in prognosis with a poor prognosis for AC-4 (Figure 3C). The AC-2 tumors had a good prognosis, suggesting a less aggressive biological phenotype prior to therapy. In contrast, AC-4 tumors express markers of a LumA phenotype before and after chemotherapy but have a poor prognosis (Figure 3C). The aggressive biology of the AC-4 tumors is not reflected in the LumA subtype of these tumors. The AC-5 group was enriched for aggressive subtypes BasalL, HER2E, or LumB in the post-NACT sample (Figures 5A and 5F), suggesting a primary resistant phenotype not affected by chemotherapy. Figure 5G summarizes the relationship between AC-subtypes and the corresponding pre-Tx and post-Tx AIMS subtypes.

To further characterize the difference between AIMS-subtyping and adaptive subtyping, we focused our analysis on those tumors with a defined AIMS subtype (LumA or LumB) as well as a defined subtype transition (LumA-to-A or LumB-to-A). As shown in Figures 6A–6D, all four subgroups defined by AIMS subtype or AIMS changes consisted of different AC-subtypes with prognostic relevance. These subtypes could not be identified by traditional intrinsic subtyping, indicating that AC-clusters provide additional prognostic information beyond pre-Tx

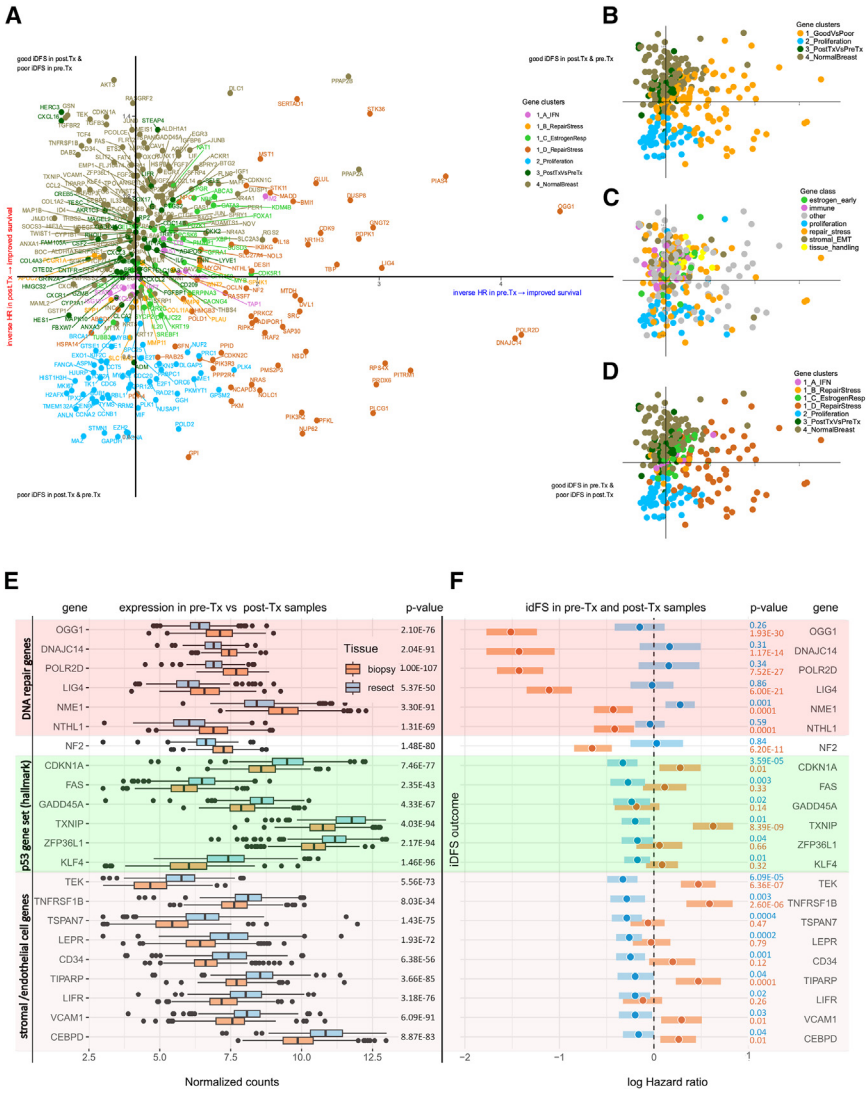

Figure 4. Differences in prognostic genes are observed in pre-Tx biopsies and post-Tx residual tumors

(A–D) Comparison of genes relevant for prognosis in pre-Tx and post-Tx samples. All 335 differentially regulated genes are displayed in a scatterplot according to their impact on disease free survival in either pre-Tx biopsies (x axis) or post-Tx resections (y axis). The inverse hazard ratio (1/HR) is shown, so that genes that are linked to improved survival in both pre-Tx and post-Tx tumors are located in the upper right quadrant. In panels A and D, the genes are color coded according to both the main gene clusters 1–4 and the subclusters (1A–1D) from the gene clustering shown in Figure 3 (with more details in Figures S4 and S5). In (B), genes are color coded only according to main gene clusters 1–4, while in (C) information from functionals pathways has been applied for color coding (complete details are given in the supplemental information).

(E) Differential expression of selected genes in pre-Tx (biopsy; orange) and post-Tx (resect; blue) samples (bars: standard error).

(F) Cox regression analysis of selected genes measured in pre-Tx (orange) and post-Tx (blue) samples, with a focus on those genes with different prognostic effects before and after neoadjuvant chemotherapy (bars: 95% CI). Also see Figures S3–S5.

AIMS subtypes and also beyond combined pre- and post-Tx subtypes.

Figures 6E–6J shows a comparison of adaptive subtyping and AIMS-based intrinsic subtyping (for pre-Tx and post-Tx samples). Important parameters for a prognostic factor are a large size of the low-risk group (Figures 6E–6G) in combination with a low event rate in this low-risk group (Figures 6H–6J). For both parameters, adaptive subtyping is superior to intrinsic subtyping: The low-risk adaptive clusters AC-1 and AC-2 cover a total of 52.77% of patients (285 of 540 patients) with a combined event rate of 2.1% (6 events in 285 patients). In contrast, the best subtype of classical intrinsic subtyping, pre-Tx LumA, covers 51% of patients but still has an event rate of 15.4%. For post-Tx subtyping, the LumA group covers 76.59% of patients, with an event rate of 22.87%. The 3-year event rates for the different subgroups are shown in Table S4.

Interaction with post-neoadjuvant palbociclib therapy

The Penelope-B trial has evaluated palbociclib compared to placebo as a post-neoadjuvant therapy. The complete trial cohort and the biomarker cohort (Figure 1C), showed no invasive disease-free survival (iDFS) survival difference between the two therapy arms. As shown in Figures S6A and S6B, the difference in prognosis of pre-Tx LumA and LumB was observed similarly in the placebo (n = 287) and the palbociclib arms (n = 307). For the post-Tx subtyping (n = 782) the prognostic difference between post-Tx LumA and B was larger in the placebo arm (Figure S6C), compared to the difference observed in the palbociclib arm (Figure S6D). However, the test for interaction was not significant in the entire cohort of post-Tx tumors. We further evaluated the four main groups of AIMS subtype changes between pre-Tx and post-Tx tumors (Figures S6E–S6I). No significant difference between treatment arms was detected for pre-Tx LumB tumors, pre-Tx LumA tumors, and post-Tx LumA tumors (Figures S6E–S6I). A significant difference (p = 0.04) between the placebo arm and the palbociclib arm was observed only in the small group of tumors (n = 48) that were LumB after NACT (post-Tx LumB tumors, Figure S6G). The prognostic relevance of the AC-subtypes was similar in the palbociclib and the placebo arm (Figures S6J and S6K), and the test for interaction between therapy arm and AC-subtypes was not significant.

Comparison of AC-subtypes with three established gene expression signatures

We compared the AC-subtypes with the three established prognostic signatures recurrence score (RS),[30] Genomic Grade Index

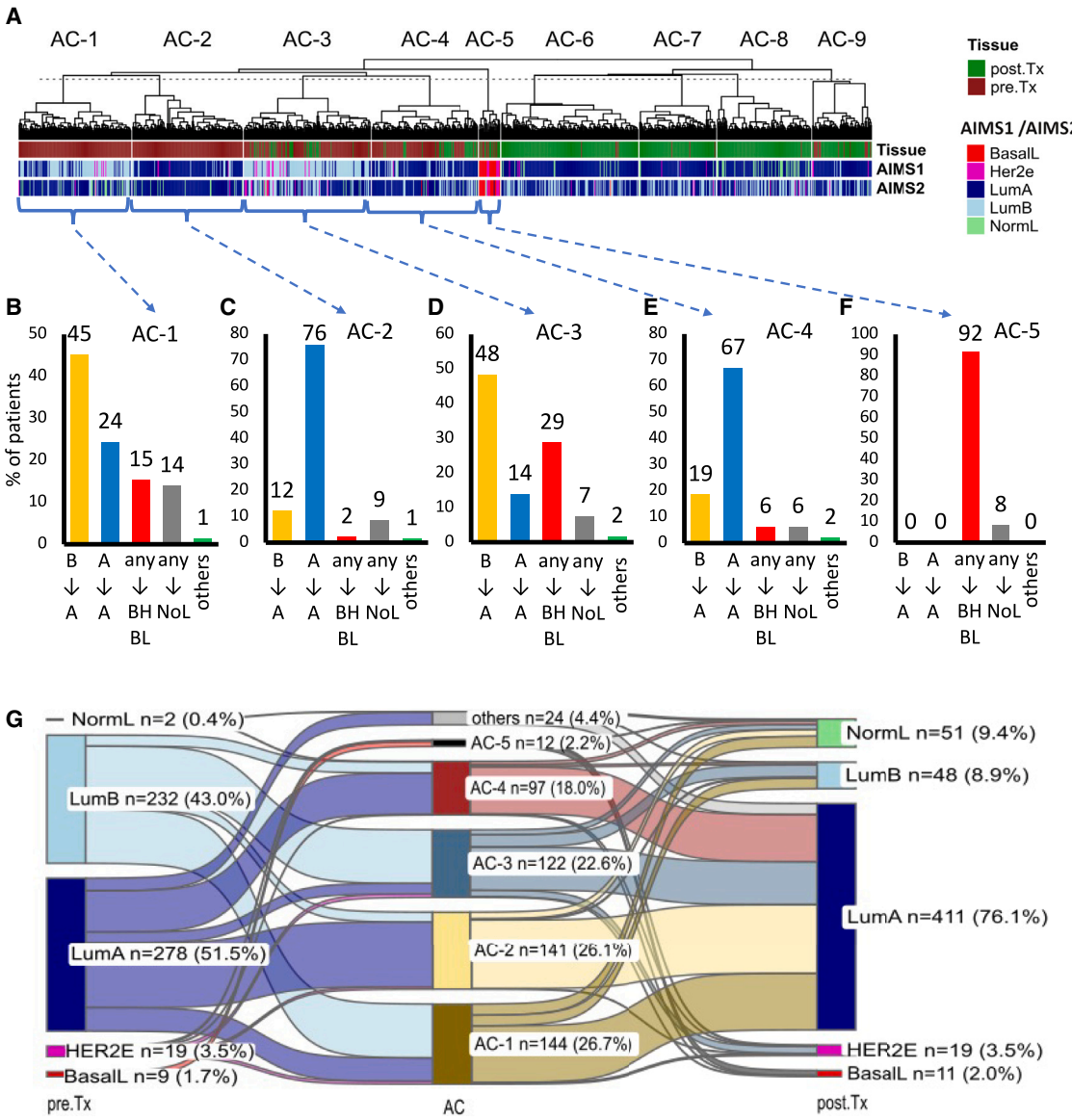

Figure 5. A systematic comparison shows that defined patterns of AIMS subtype adaptation during neoadjuvant chemotherapy are reflected in the different AC subtypes

(A) Distribution of AIMS subtypes for individual tumors based on the combined heatmap (as shown in Figure 3) AIMS1: Aims subtype of the primary sample (either biopsy or resection), AIMS2: subtype of paired corresponding sample.

(B–F) Different patterns of subtype transition and adaptation during neoadjuvant chemotherapy in the five different adaptive clusters, AC-1 (B), AC-2 (C), AC-3 (D), AC-4 (E), and AC-5 (F); with very similar patterns in AC-1 and AC-3 (both mainly LumB-to-A) as well as in AC-2 and AC-4 (both mainly LumA-to-A). AC-5 consists mainly of highly aggressive HER2E and BasalL subtypes. (abbreviations: A = LumA; B=LumB; BHBL = LumB+HER2E + BasalL; NoL = NormL).

(G) Sankey diagram showing the grouped pre- and post-Tx AIMS subtypes of 540 patients with the corresponding AC-groups.

(GGI),[31] and the Sensitivity to Endocrine Therapy Index (SET).[32] These signatures were selected because RS is an established molecular diagnostic test, GGI is a prototype of a proliferation-related signature and SET is an important endocrine-response related signature.

We have transferred the genes of the three signatures to the HTG system (Figure S7), defined three Penelope-B patient groups for each signature based on tertiles, and evaluated the performance of the AC-subtypes from Figure 3C in these tertiles. The three gene expression signatures itself are prognostic in the Penelope-B cohort (Figures 7A–7C). As expected, RS and GGI showed a high correlation with the proliferation gene cluster 2 and SET with the estrogen-response gene cluster 1C (Figure 7D). The correlation of the three signatures with gene cluster 1, in particular with subcluster 1D, that provides the most prognostic information in the Penelope-B cohort is very limited (Figure 7D). If we focus on patient groups defined by high, low, or intermediate RS, GGI, or SET, we could show that in each of these groups, the AC-clusters provide highly significant prognostic information (all p values < 0.0001; Figures 7E–7G).

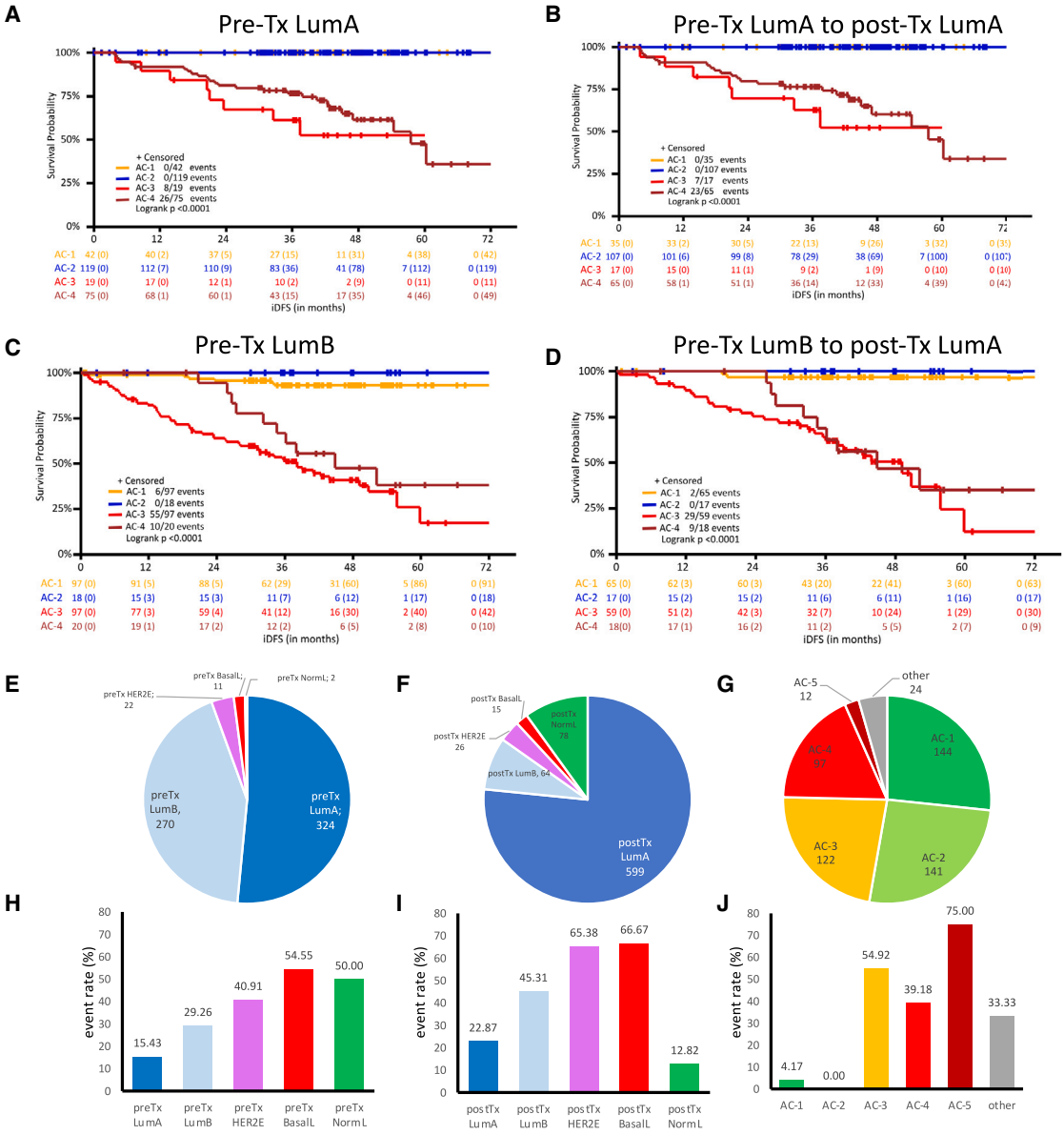

Figure 6. AC-clusters provide additional prognostic information beyond pre-Tx AIMS subtypes and also beyond combined pre- and post-Tx subtypes

(A–D) Prognostic relevance of AC clusters in homogeneous AIMS subtypes (A) AC-subtypes in 255 baseline LumA tumors; (B) AC-subtypes in 224 LumA-to-A tumors; (C) AC-subtypes in 232 baseline LumB tumors; (D) AC-subtypes in 159 LumB-to-A tumors. AC-clusters are shown based on the clustering in Figure 3.
(E–G) Prevalence of the different subtypes for (E) pre-Tx AIMS (n = 629), (F) post-Tx AIMS (n = 782) as well as (G) adaptive subtyping (n = 540).
(H–J) Event rate for iDFS in the different subtypes for (H) pre-Tx AIMS, (I) post-Tx AIMS as well as (J) adaptive subtyping. See also Table S4.

UMAP as an additional statistical approach

From a bioinformatical point of view, one of the most interesting findings of our study was that the focus on 335 DEGs in pre-Tx vs. post-Tx tumor samples allowed the identification of highly significant prognostic groups by a comparably simple clustering analysis (Figure 3). To reconfirm and validate that this prognostic information can be generated based on gene expression information, we repeated the analysis using uniform manifold approximation and projection (UMAP)[33,34] as an independent method for dimension-reduction. As shown in Figure 8, a UMAP of 1,080 patient samples resulted in a separation of pre-Tx and post-Tx samples as well as in the separation of three UMAP clusters within the pre-Tx sample cohort (Figure 8A). The UMAP clusters are distinct from the classical LumA vs. LumB subtypes (color coding in Figure 8A), but they show a considerable overlap with the AC-Subtypes (color coding in Figure 8B), with a clear separation of the good prognosis AC-1 and AC-2 subtypes in the UMAP analysis. The three UMAP clusters (Figure 8C) show differences in patient prognosis (Figure 8D), with an excellent prognosis of UMAP-cluster 1.

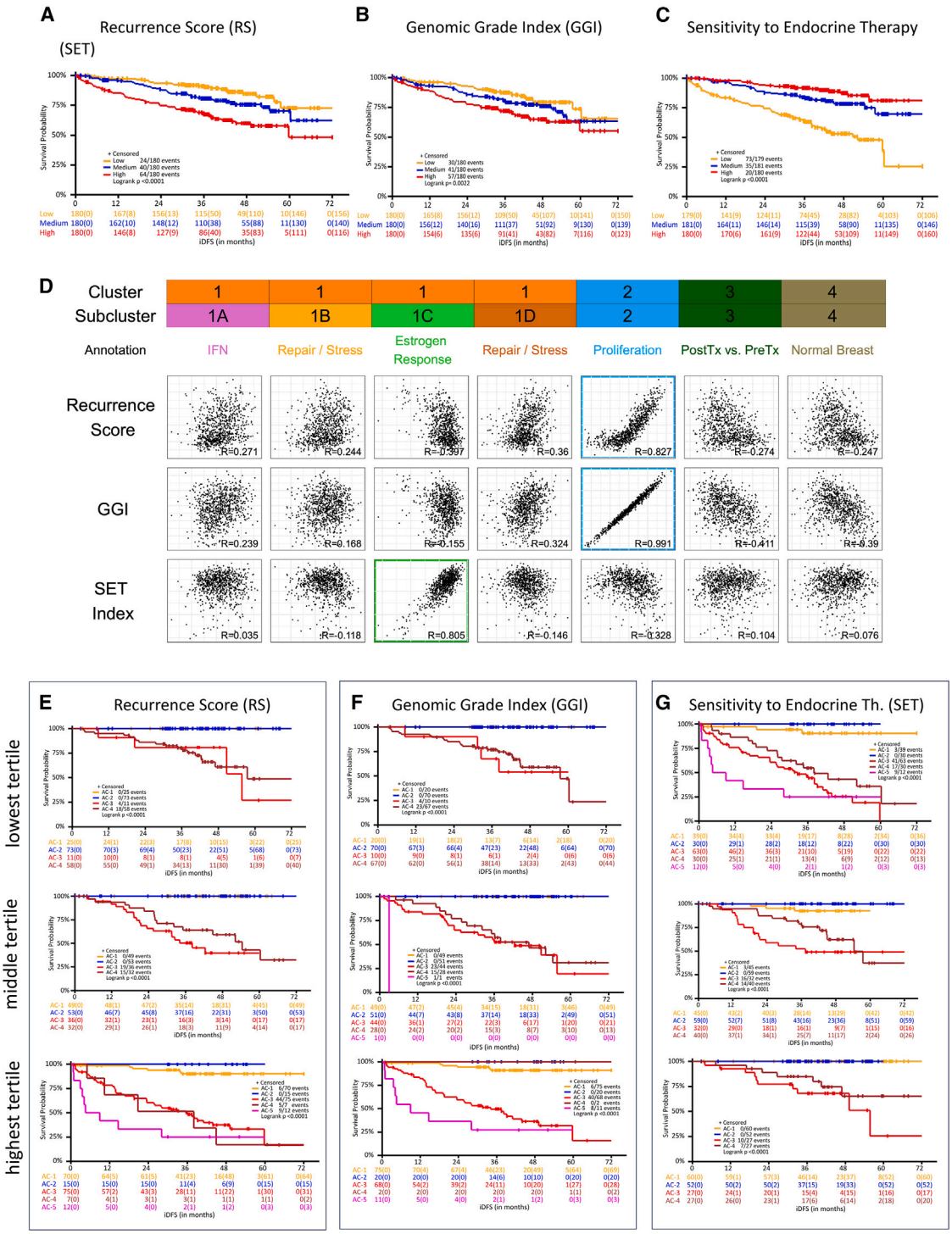

Figure 7. AC-subtypes provide significant prognostic information in comparison with three established gene signatures in breast cancer (recurrence score (RS), Genomic Grade Index (GGI) and Sensitivity to Endocrine Therapy Index (SET)

(A–C) Prognostic relevance of RS (A), GGI (B), and SET (C) in the Penelope-B cohort (n = 540). Each gene expression signature is divided into three tertiles (high, intermediate and low risk), these groups are prognostic in the Penelope-B cohort, with high significance for RS and SET ($p < 0.001$) and moderate significance for GGI ($p = 0.02$).

(D) Comparison of the main Penelope-derived gene clusters with the three established gene signatures RS, GGI and SET. The gene clusters from the Penelope-B analysis (as shown in Figure 3) were analyzed in RNA-seq data of 812 ER positive breast cancer samples from TCGA for their correlation to established gene signatures (recurrence score, GGI, and SET-index) as shown in the scatterplots. Scatterplots with Pearson correlation values R > 0.5 are highlighted: Both recurrence score (R = 0.827) and GGI (R = 0.991) display strong correlation with gene cluster 2 (cell cycle/proliferation) from the Penelope-B analysis. Subcluster

(legend continued on next page)

Evaluation in independent biopsies from Penelope-B as well as the SCAN-B cohort

A total of 89 pre-Tx samples from Penelope-B had not been used in the analysis that identified the AC-1 to AC-5 subgroups, because these samples did not have a paired post-Tx tumor sample. We used these independent 89 pre-Tx samples as an additional cohort to evaluate the prognostic relevance of the centroid-based AC-subgroups. This small independent cohort showed a similar prognostic result as the training cohort (Figure S8A), the analysis of the complete cohort of 629 pre-Tx samples is shown for comparison in Figure S8B.

In addition, we performed a survival analysis of centroid-based AC-clusters in a cohort of 3,764 ER+ Her2- tumors from the SCAN-B cohort[35] (Figures S8C and S8D, with an enlarged y axis in D to show minor differences between AC-subtypes). The main limitation of the SCAN-B analysis is the low event rate of only 222 events in 3,764 patients (5.9%), which is much lower compared to the high-risk Penelope-B cohort. The AC-5 subgroup shows a poor prognosis also in SCAN-B. There are minor prognostic differences between AC-2 and AC-4, with an improved prognosis for AC-2, similar to Penelope-B. The AC-3 subtype, which shows a LumB to A transition during neoadjuvant therapy in the Penelope-B cohort, is not observed in SCAN-B.

DISCUSSION

The main findings of our investigation are that (1) classical breast cancer subtypes are not stable under therapeutic pressure, (2) that therapy-induced molecular adaptation provides new options for classification of breast cancer using the adaptive clusters (AC-1-5), and (3) that a subset of genes, particularly genes from DNA repair related pathways, have a strong positive prognostic role predominantly in the pre-Tx biopsies.

Intrinsic subtyping of breast cancer is the state-of-the-art approach to identify different subtypes.[36] Previous prognostic and predictive approaches have mainly evaluated biomarkers in pretherapeutic biopsies.[8,37] In research, serial biopsies before and after treatment have been used both in breast cancer[38–40] as well as other cancer types.[41–44] In breast cancer this approach has been especially useful in the context of neoadjuvant trials of both endocrine therapy[24,45–48] and adaptive neoadjuvant chemotherapy regimens.[25,49,50]

For interpretation of our results, it is important to appreciate that the post-neoadjuvant Penelope-B cohort is a highly selected patient cohort comprised of tumors with an aggressive biology and a high tumor stage before and after NACT (measured as part of the CPS-EG score). All tumors were treated with neoadjuvant chemotherapy regimens, and all had residual disease after NACT. This cohort allows us to focus on high-risk patients with a need for improved clinical strategies, but it is also a limitation for validation in other clinical cohorts.

An important result is the finding that a therapy-induced transition between LumA and LumB subtypes is common in breast cancer treated with neoadjuvant therapy. For subclonal mutations, it has been shown that they are present already before NACT,[51] suggesting that the potential to adjust the subtype during chemotherapy and in metastatic disease is present in the primary biopsy. Aggressive subclones in a tumor are reduced during NACT, which is observed as a LumB-to-A transition. But in some tumors, the aggressive subclones may regrow as LumB metastatic disease. However, it should be emphasized that the positive prognostic impact of the post-NACT LumA phenotype as well as the LumB-to-A transition suggests that the reverse transition to LumB is only relevant in the small subset of patients with metastatic disease. The presence and absence of aggressive subclones could also explain the different prognostic value of the identified genes in pre- and post-Tx tumors.

As a result of this clonal selection process induced by therapeutic pressure, a metastatic breast cancer cohort could be very different from an early breast cancer cohort. Interestingly, we observed an effect of palbociclib in the small group of tumors that remained LumB after NACT, the subtype that is enriched in metastatic biopsies. This observation could contribute to the explanation why a metastatic cohort, as treated in the Paloma-3 study,[52] might respond differently to CDK4/6 inhibitors, compared to a post-NACT or adjuvant cohort, as treated in Penelope-B[26] and Pallas.[53,54]

While most of the tumors in the HR+/HER2- Penelope-B cohort were LumA or LumB, our study has also identified a small group of BasalL or HER2E tumors with particularly poor outcomes, which is clinically relevant to identify patients for more aggressive therapy approaches, including combinations of immunotherapy and chemotherapy, as investigated in the KN-756[19] and the Checkmate7FL.[20] In a previous study of 16 pairs of primary tumor and metastasis, all metastases had the identical subtype as the primary tumor, but in this cohort, the majority of samples were non-luminal and there was only one pair of luminal tumors.[55]

In our study, we used paired biopsies to identify the genes that are relevant for adaptive clustering. Once these genes were identified, however, the prediction for new samples could be done using a centroid-based classifier on the pretherapeutic biopsy, suggesting that the prognostic biological program is already present in the pre-Tx samples.

We focused on intra-tumoral, therapy-induced longitudinal heterogeneity by identifying those genes that are differentially expressed before and after therapy in paired samples. Clustering of tumors based on these genes improved information about long-term outcome after neoadjuvant chemotherapy. The results were very similar using the cluster analysis that was the main bioinformatical approach as well as the additional UMAP analysis, indicating that different methods for dimension-reduction lead

1C from the Penelope-analysis which was characterized by estrogen responsive genes displays a strong correlation (R = 0.805) with the SET-index. Calculation of RS[30] and GGI[31] were adapted from genefu package[67], and SET[32] from Sinn 2019.[68] Detailed code is provided in the supplemental information.
(E–G) The AC-subtyping derived from Figure 3C (n = 516) was tested in three groups for each established signature (high, intermediate, low; based on tertiles for RS, GGI, and SET). The AC-clusters were highly significant in all 9 subgroups (p <0 .0001). (E) AC-subtypes in three risk groups based on RS (top: low risk tertile, middle: intermediate risk tertile, low: high risk tertile). (F) AC-subtypes in three risk groups based on GGI (top: low risk tertile, middle: intermediate risk tertile, low: high risk tertile). (G) AC-subtypes in three risk groups based on SET (top: high risk tertile, middle: intermediate risk tertile, low: low risk tertile). For the SET index, the high-risk patient group is included in the SET low tertile, because SET has an inverse scale. See also Figure S7.

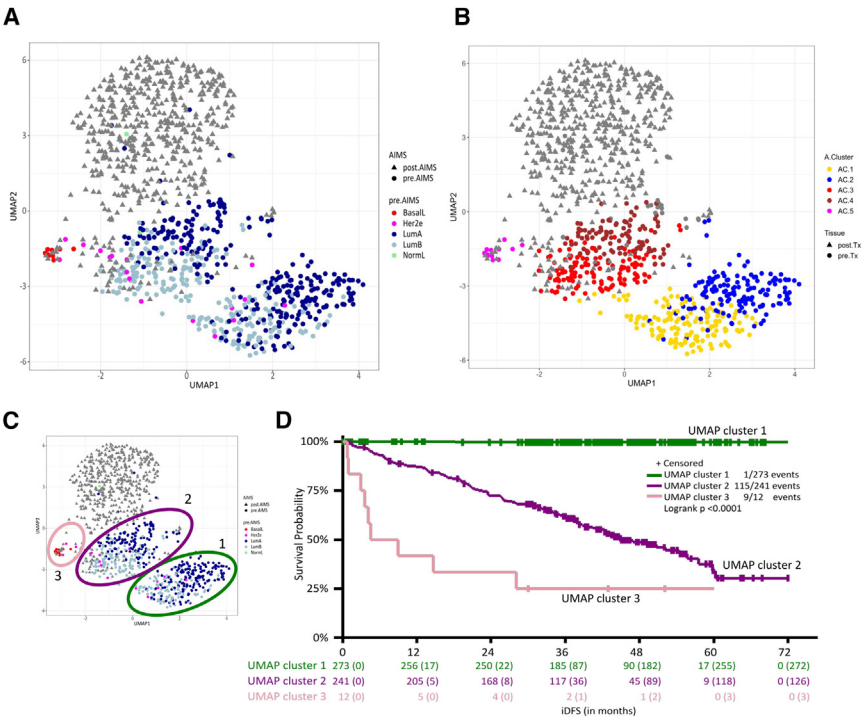

Figure 8. An independent dimension reduction by UMAP analysis based on 335 differentially expressed genes identifies similar prognostic subgroups as the adaptive cluster analysis

(A) A UMAP was generated for 1080 tumor samples (540 paired pre- and post-Tx samples) with euclidean metric for the set of 335 DEGs between pre-Tx and post-TX samples. As shown in (A), post-Tx samples (gray triangles) are separated from the pre-Tx samples (dots). Within the pre-Tx samples, there are three clearly separated groups: one small group of BasalL tumors (red) and two larger groups, each of them consisting of a mixture of LumA (dark blue) but also LumB (light blue) tumors. Therefore, this UMAP based classification is different from the traditional intrinsic subtypes.

(B) Identical UMAP as in (A) with different color-coding representing the 5 AC-subtypes. The good prognosis AC-subtypes AC-1 and AC-2 are combined in one cluster, while the poor prognosis subtypes AC-3 and AC-4 are combined in the second main cluster.

(C and D) Kaplan-Meier analysis of 526 pre-Tx tumors included in the UMAP clusters 1, 2, and 3 (C), with very good prognosis for tumors in cluster 1. The UMAP analysis shows that once the 335 differentially expressed genes are identified, prognostic groups become evident that are not covered by the LumA and LumB classification. See also Figure S8.

to similar results, if the analysis is based on differentially expressed genes. The adaptive subtypes have an additional prognostic value that goes beyond AIMS subtyping. They are also different from the established gene expression signatures RS, GGI, and SET. These three gene expression signatures are prognostic in the Penelope-B cohort, but the AC-clusters add additional prognostic information in patient subgroups within three tertiles defined by RS, GGI, or SET.

Using this approach, we defined five adaptive clusters in the Penelope-B cohort: Two clusters (AC-1 and AC-2), containing more than half of the patients within the cohort, have an excellent prognosis. In contrast, tumors within the AC-3, AC-4, and AC-5 subgroups have high event rates of 55%, 39%, and 75%, respectively, suggesting that the AC clustering is able to identify those tumors with an aggressive biology. Of the five AC-subtypes, only the AC-5 group has a high overlap with already known BasalL/HER2E subtype. For the other four subtypes AC-1 to AC-4, the prognostic effects cannot be explained by an association with LumA or LumB phenotypes. The AC-2 vs. AC-4 subgroups are very similar regarding the classical intrinsic subtypes; the majority of these tumors have a LumA subtype that remains LumA after chemotherapy (LumA-to-A). However, AC-2 has an excellent prognosis and AC-4 has a poor prognosis. This suggests that even in consistently LumA tumors there are aggressive subsets that contribute to poor outcome. Likewise, the AC-1 vs. AC-3 subtypes have major differences in patient prognosis but a very similar LumB-to-A phenotype. The prognostic differences within this LumB-to-A subgroup can only be identified by AC-clustering and may be relevant for patient therapy strategies.

The most relevant prognostic differences between AC-1/AC1 vs. AC3/AC-4 are mainly driven by the genes in gene cluster 1, which includes highly prognostic genes involved in DNA-repair and chemotherapy response, including *OGG1*,[56] *DNAJC14*,[57] *POLR2D*,[58] *LIG4*,[59] *NME1*,[60] and *NTHL1*.[61] Interestingly, these genes are among the genes with the highest positive prognostic impact of all genes investigated in pre-Tx biopsies, suggesting that a pre-Tx activation of DNA-repair genes (indicating genomic instability) might be a good basis for reduction of aggressive cell clones by neoadjuvant chemotherapy, even in the setting of a non-pCR.

Limitations of the study

Limitations of our study include the ongoing follow-up, the restricted biomaterial in pre-Tx samples and the inclusion of only no-pCR patients. The pCR rate in HR+/Her2- tumors is typically comparably low, but this limitation needs to be considered for future validation approaches. Penelope-B has used the CPS-EG system[27,62] and data on residual cancer burden (RCB)[18] is not available. For comparison of pre-Tx and post-Tx samples, it is important to realize that that some genes are known to be artificially induced by surgery.[63,64] An additional validation of the AC-subtypes is currently challenging, because there are no similar cohorts available for high-risk HR-positive breast cancers non-responding to NACT. This is evident from the analysis of AC-subtypes in the SCAN-B cohort, which showed a poor prognosis of AC-5 as well as some prognostic differences between AC-2 and AC-4 but could not address the difference between AC-1 and AC-3, suggesting that a prior neoadjuvant therapy inducing a LumB-to-A phenotypic switch might be relevant for those subtypes. SCAN-B is predominantly a cohort of tumors treated with adjuvant therapy, which excludes an adaptation of tumors from LumB-to-LumA during the neoadjuvant phase. Penelope-B did

not show a statistically significant benefit of post-neoadjuvant palbociclib, in contrast to the high efficacy in the metastatic setting.[52,65] However, the small group of patients with LumB tumors after NACT (n = 48) potentially derived benefit from palbociclib, which needs to be validated in additional cohorts.[49]

In summary, we have shown that classical breast cancer subtypes can change during neoadjuvant chemotherapy, predominantly from LumB to LumA. While post-Tx LumA tumors have an improved prognosis as a group, a change back to LumB is observed in metastatic disease, which could be explained by re-expansion of aggressive and resistant cell clones. Based on a systematic comparison of longitudinal samples before and after chemotherapy, we have identified additional adaptive clusters (AC-1 to AC-5) of breast cancer. The AC-subtypes could be a basis for new therapeutic strategies and for more precise assessment of patient prognosis. These therapeutic strategies might include additional post-neoadjuvant treatment options (e.g., with antibody-drug conjugates or post-neoadjuvant chemotherapy), intensified neoadjuvant treatment (e.g., with addition of neoadjuvant immunotherapy) as well as modified neoadjuvant and post-neoadjuvant concepts involving agents that specifically target DNA repair, including PARP inhibitors. These results need to be validated in additional high-risk cohorts, for example in ongoing post-neoadjuvant trials.

RESOURCE AVAILABILITY

Lead contact

Further information and requests for resources and reagents should be directed to and will be fulfilled by the lead contact, Sibylle Loibl (sibylle.loibl@gbg.de).

Materials availability

This study did not generate new unique reagents.

Data and code availability

- The RNA expression data from pre-Tx, post-Tx, and metastatic samples for this study has been uploaded on both GitHub and Zenodo. This includes the normalized HTG RNA expression data for all 2,549 genes together with de-identified patient baseline data that is available online with access for all readers of the manuscript. The original analysis code as well as the output files have been deposited on GitHub and Zenodo and is publicly available as of the date of publication. All accession numbers are listed in the key resources table.
- Any additional information required to reanalyze the data reported in this paper is available Dynamics of molecular heterogeneity in breast cancer from the lead contact upon request.

ACKNOWLEDGMENTS

The analysis was partly funded by the German Cancer Aid (#70113450) as well as BMBF (#01KD2206M; SATURN3). Research and biostatistical resources were provided by GBG and clinical trial funding was provided by Pfizer. We would like to thank all patients, clinicians and pathologists participating in the clinical studies and the biomaterial collection as well as the team at the GBG Headquarters and GBG Biobank at the Institute of Pathology, Philipps-University Marburg.

AUTHOR CONTRIBUTIONS

The study was designed by C.D., S.R., T.K., K.W., J.H., V.N., and S.L.; C.D., M.M., F.M., M.U., H.B., S.-B.K., S.S., H.D.B., A.K.W., S.-A.I., A.DeM., A.P., L.v.V., N.McC., T.S., P.J., K.A.G., J.A.G.-S., C.C.W., C.M.K., T.R., B.F., M.M.O., E.S.K., N.T., F.R., W.D.S., P.A.F., J.T.-S., Z.Z., H.S.R., M.G., A.M., and S.L. contributed to data acquisition; data analysis was performed by C.D., S.R., T.K., K.W., V.N., and S.L.; patient recruitment, sample and data collection was performed by C.D., M.M., F.M., M.U., H.B., S.-B.K., S.S., H.D.B., A.K.W., S.-A.I., A.DeM., A.P., L.v.V., N.McC., T.S., P.J., K.A.G., J.A.G.-S., C.C.W., C.M.K., T.R., B.F., M.M.O., E.S.K., N.T., F.R., W.D.S., P.A.F., J.T.-S., Z.Z., H.S.R., M.G., A.M., J.H., and S.L. All authors interpreted the data. The first draft of the report was written by C.D. Verification of the underlying data was performed by S.R. and C.D. The decision to submit the report for publication was made by all the authors. All authors contributed to the review of the manuscript.

DECLARATION OF INTERESTS

C.D. reports grants from EU-H2020, BMBF, German Cancer Aid, and GBG, during the conduct of the study; personal fees from Novartis, Roche, MSD Oncology, DaiichiSankyo, Merck, AstraZeneca, and MolecularHealth; and institutional grants from Myriad, outside the submitted work. C.D. has a patent VMscope digital pathology software with royalties paid, a patent application related to prognostic subtypes in high-risk luminal breast cancer pending, as well as patents WO2020109570A1 and WO2015114146A1 pending and WO2010076322A1, issued. S.R., K.W., S.S., B.F., and V.N. report institutional grants from DaiichiSankyo, Gilead, Novartis, Pfizer, Roche, Seagen during the conduct of this work and from AbbVie, AstraZeneca, BMS, DaiichiSankyo, MolecularHealth, Novartis, Roche, Pfizer outside this work. S.R., K.W., S.S., B.F., and V.N. declare to be GBG Forschungs GmbH employees; GBG Forschungs GmbH royalties/patents: EP14153692.0, EP21152186.9, EP15702464.7, and EP19808852.8 and VM Scope GmbH as well as a patent application related to prognostic subtypes in high-risk luminal breast cancer pending. T.K. declares a patent application related to prognostic subtypes in high-risk luminal breast cancer pending. M.U. reports consulting fees to the institution from AstraZeneca, DaiichiSankyo, Lilly, MSD Merck, Myriad Genetics, Novartis, Pierre Fabre, Pfizer, Gilead, Roche, Sanofi Aventis, Seagen, Stemline, CD Pharma and honoraria to the institution from Astra Zeneca, Daiichi Sankyo, Lilly, Myriad Genetics, Novartis, Pierre Fabre, Pfizer, Roche, Sanofi Aventis, Stemline, all outside the submitted work. S.-B.K. reports institutional grants from Novartis and Sanofi-Aventis, personal consulting fees from AstraZeneca, Beigene, DaeHwah Pharma, DaiichiSankyo, Ensol Bioscience Inc, ISU Abxis, Lilly, Novartis, OBI Pharma, and stock/stock options from Genopeaks and Neogene TC, all outside this work. H.D.B. reports stock ownership from Pfizer, Abbvie. and Viatris and research support from Merck Sharp & Dohme. N.McC. reports travel support from Novartis, AstraZeneca, Gilead, and Merck and participation in data safety or advisory board from Novartis, Gilead and Merck, outside the submitted work. C.C.W. is supported by the postdoctoral lecture qualification program of the Anneliese Pohl Foundation, Marburg. C.M.K. reports travel support from Novartis. T.R. reports institutional grants from German Cancer Aid, Else Kroener Fresenius Foundation, and German Society of Senology, outside this work and personal fees and travel support from Pfizer. M.M.O. reports travel support from Lilly and Novartis outside this work. E.S.K. reports institutional grants from NIH/NCI, Blueprint Medicine, and Bristol Meyer Squibb, personal consulting fees from Aleksia Pharmaceutical and Cancer Cell Cycle-LLC, and receipt of materials from Incyclix Pharma, all outside this work. N.T. reports consulting fees from Astra Zeneca, Lilly, Pfizer, Roche/Genentech, Novartis, GlaxoSmithKline, Repare therapeutics, Relay therapeutics, Gilead, Inivata, Guardant, and Exact Sciences and grants from AstraZeneca, Pfizer, Roche/Genentech, Merck Sharpe and Dohme, Guardant Health, Invitae, Inivata, Personalis, and Natera, all outside of this work. F.R. reports consulting fees from BMS, Astra Zeneca, Roche, and MSD and honoraria and travel support from Novartis, Amgen, and Menarini, all outside this work. W.D.S. reports honoraria from AstraZeneca, GlaxoSmithKline, NOGGO, and Roche outside this work. P.A.F. reports institutional grants Biontech, Cepheid, and Pfizer; personal consulting fees and honoraria from Novartis, Pfizer, Roche, Daiichi-Sankyo, AstraZeneca, Lilly, Eisai, Merck Sharp & Dohme, Pierre Fabre, SeaGen, Agendia, Sanofi Aventis, Gilead, and Mylan; and participation in data safety monitoring boards or advisory boards for Novartis, Pfizer, Roche, Daiichi-Sankyo, AstraZeneca, Lilly, Eisai, Merck Sharp & Dohme, Pierre Fabre, SeaGen, Agendia, Sanofi Aventis, Gilead, and Mylan, all outside this work. M.T. reports research grants from Chugai,

Takeda, Pfizer, Taiho, JBCRG assoc., KBCRN assoc., Eisai, Eli-Lilly and companies, Daiichi-Sankyo, AstraZeneca, Astellas, Shimadzu, Yakult, Nippon Kayaku, AFI technology, Luxonus, Shionogi, GL Science, and Sanwa Shurui and honoraria from Chugai, Takeda, Pfizer, Kyowa-Kirin, Taiho, Eisai, Daiichi-Sankyo, AstraZeneca, Eli Lilly, MSD, Exact Science, Novartis, Shimadzu, Yakult, Nippon Kayak, Devicore Medical Japan, Sysmex and participation in monitoring and advisory boards for Daiichi-Sankyo, Eli Lilly, BMS, Bertis, Terumo, Kansai Medical Net. He reports board membership for Assoc. JBCRG, Assoc. OOTR, Assoc. KBCRN, Assoc. JBCS and associate editorship for British Journal of Cancer, Scientific Reports, Breast Cancer Research and Treatment, Cancer Science, Asian Journal of Surgery, and Asian Journal of Breast Surgery, all outside this work. M.G. reports personal consulting fees for EliLilly, MSD, Novartis, Menarini-Stemline and honoraria from AstraZeneca, DaiichiSankyo, EliLilly, EPQHealth, Novartis, PierreFabre; payment for expert testimony from Veracyte and travel support from EliLilly and Novartis, leadership for ABCSG GmbH and ABCSG Research GmbH and other for Sandoz GmbH. A.M. reports honoraria for lectures from Pfizer. J.H. reports institutional grants from DaiichiSankyo, Gilead, Novartis, Pfizer, Roche, and Seagen during the conduct of this work and from AbbVie, AstraZeneca, BMS, DaiichiSankyo, MolecularHealth, Novartis, Roche, and Pfizer outside this work. J.H. reports personal consulting fees from MSD Oncology, Novartis, Palleos Health Care, Pfizer, Roche Pharma, and Seagen and honoraria from Daiichi-Sankyo, Gilead, Novartis, Pfizer, and Roche Pharma, Seagen and non-financial support from Hologic, all outside this work. J.H. declares to be GBG Forschungs GmbH employee; GBG Forschungs GmbH has royalties/patents: EP14153692.0, EP21152186.9, EP15702464.7, EP19808852.8, and VM Scope GmbH. S.L. reports grants to the institution from AbbVie, AstraZeneca, Celgene, Daiichi-Sankyo, Immunomedics/Gilead, Molecular Health, Novartis, Roche, and Pfizer. S.L. declares to be GBG Forschungs GmbH employee; GBG Forschungs GmbH has following royalties/patents: EP14153692.0, EP21152186.9, EP15702464.7, EP19808852.8, and VM Scope GmbH as well as a patent application related to prognostic subtypes in high-risk luminal breast cancer pending; honoraria for lectures and presentations from AstraZeneca, DSI, Gilead, Pfizer, Novartis, Roche, Seagen, and Medscape as well as honoraria for advisory boards from Abbvie, Amgen, AstraZeneca, BMS, Celgene, DSI, EirGenix, Gilead, GSK, Lilly, Novartis, Merck, Olema, Pfizer, Pierre Fabre, Relay Therapeutics, Roche, and Seagen. S.L. reports non-financial interest as advisory role in AGO Kommission Mamma, as principal investigator (Aphinity), as member in AGO, ASCO, DKG, ESMO, and other non-financial interest from AstraZeneca, Daiichi-Sankyo, immunomedica/Gilead, Novartis, Pfizer, Roche, and Seagen.

STAR★METHODS

Detailed methods are provided in the online version of this paper and include the following:

- KEY RESOURCES TABLE
- EXPERIMENTAL MODEL AND STUDY PARTICIPANT DETAILS
  - Study design and clinical cohorts
- METHOD DETAILS
  - Endpoints
  - Biobanking and central pathology
  - Gene expression analysis in pre-therapeutic and post-therapeutic samples
  - Molecular analyses – AIMS subtypes
  - Differential gene expression analysis, clustering and UMAP analysis
  - Gene set enrichment analysis
  - Generation of centroids
  - Evaluation of the existing gene signatures recurrence score, GGI, SET index
  - Evaluation of SCAN-B cohort
- QUANTIFICATION AND STATISTICAL ANALYSIS

SUPPLEMENTAL INFORMATION

Supplemental information can be found online at https://doi.org/10.1016/j.ccell.2025.01.002.

Received: April 26, 2024
Revised: January 9, 2025
Accepted: January 9, 2025
Published: January 30, 2025

REFERENCES

1. Perou, C.M., Sørlie, T., Eisen, M.B., van de Rijn, M., Jeffrey, S.S., Rees, C.A., Pollack, J.R., Ross, D.T., Johnsen, H., Akslen, L.A., et al. (2000). Molecular portraits of human breast tumours. Nature *406*, 747–752. https://doi.org/10.1038/35021093.
2. Sørlie, T., Perou, C.M., Tibshirani, R., Aas, T., Geisler, S., Johnsen, H., Hastie, T., Eisen, M.B., van de Rijn, M., Jeffrey, S.S., et al. (2001). Gene expression patterns of breast carcinomas distinguish tumor subclasses with clinical implications. Proc. Natl. Acad. Sci. USA *98*, 10869–10874. https://doi.org/10.1073/pnas.191367098.
3. Goldhirsch, A., Wood, W.C., Coates, A.S., Gelber, R.D., Thürlimann, B., and Senn, H.J.; Panel members (2011). Strategies for subtypes–dealing with the diversity of breast cancer: highlights of the St. Gallen International Expert Consensus on the Primary Therapy of Early Breast Cancer 2011. Ann. Oncol. *22*, 1736–1747. https://doi.org/10.1093/annonc/mdr304.
4. Denkert, C., von Minckwitz, G., Brase, J.C., Sinn, B.V., Gade, S., Kronenwett, R., Pfitzner, B.M., Salat, C., Loi, S., Schmitt, W.D., et al. (2015). Tumor-infiltrating lymphocytes and response to neoadjuvant chemotherapy with or without carboplatin in human epidermal growth factor receptor 2-positive and triple-negative primary breast cancers. J. Clin. Oncol. *33*, 983–991. https://doi.org/10.1200/JCO.2014.58.1967.
5. Metzger-Filho, O., Collier, K., Asad, S., Ansell, P.J., Watson, M., Bae, J., Cherian, M., O'Shaughnessy, J., Untch, M., Rugo, H.S., et al. (2021). Matched cohort study of germline BRCA mutation carriers with triple negative breast cancer in brightness. NPJ Breast Cancer *7*, 142. https://doi.org/10.1038/s41523-021-00349-y.
6. Wolf, D.M., Yau, C., Wulfkuhle, J., Brown-Swigart, L., Gallagher, R.I., Lee, P.R.E., Zhu, Z., Magbanua, M.J., Sayaman, R., O'Grady, N., et al. (2022). Redefining breast cancer subtypes to guide treatment prioritization and maximize response: Predictive biomarkers across 10 cancer therapies. Cancer Cell *40*, 609–623.e6. https://doi.org/10.1016/j.ccell.2022.05.005.
7. Loibl, S., André, F., Bachelot, T., Barrios, C.H., Bergh, J., Burstein, H.J., Cardoso, M.J., Carey, L.A., Dawood, S., Del Mastro, L., et al. (2024). Early breast cancer: ESMO Clinical Practice Guideline for diagnosis, treatment and follow-up. Ann. Oncol. *35*, 159–182. https://doi.org/10.1016/j.annonc.2023.11.016.
8. Andre, F., Ismaila, N., Allison, K.H., Barlow, W.E., Collyar, D.E., Damodaran, S., Henry, N.L., Jhaveri, K., Kalinsky, K., Kuderer, N.M., et al. (2022). Biomarkers for Adjuvant Endocrine and Chemotherapy in Early-Stage Breast Cancer: ASCO Guideline Update. J. Clin. Oncol. *40*, 1816–1837. https://doi.org/10.1200/JCO.22.00069.
9. Cardoso, F., van't Veer, L.J., Bogaerts, J., Slaets, L., Viale, G., Delaloge, S., Pierga, J.Y., Brain, E., Causeret, S., DeLorenzi, M., et al. (2016). 70-Gene Signature as an Aid to Treatment Decisions in Early-Stage Breast Cancer. N. Engl. J. Med. *375*, 717–729. https://doi.org/10.1056/NEJMoa1602253.
10. Sparano, J.A., Gray, R.J., Makower, D.F., Pritchard, K.I., Albain, K.S., Hayes, D.F., Geyer, C.E., Jr., Dees, E.C., Goetz, M.P., Olson, J.A., Jr., et al. (2018). Adjuvant Chemotherapy Guided by a 21-Gene Expression Assay in Breast Cancer. N. Engl. J. Med. *379*, 111–121. https://doi.org/10.1056/NEJMoa1804710.
11. Filipits, M., Rudas, M., Jakesz, R., Dubsky, P., Fitzal, F., Singer, C.F., Dietze, O., Greil, R., Jelen, A., Sevelda, P., et al. (2011). A new molecular predictor of distant recurrence in ER-positive, HER2-negative breast cancer adds independent information to conventional clinical risk factors. Clin. Cancer Res. *17*, 6012–6020. https://doi.org/10.1158/1078-0432.CCR-11-0926.

12. Parker, J.S., and Perou, C.M. (2015). Tumor Heterogeneity: Focus on the Leaves, the Trees, or the Forest? Cancer Cell *28*, 149–150. https://doi.org/10.1016/j.ccell.2015.07.011.

13. Zardavas, D., Irrthum, A., Swanton, C., and Piccart, M. (2015). Clinical management of breast cancer heterogeneity. Nat. Rev. Clin. Oncol. *12*, 381–394. https://doi.org/10.1038/nrclinonc.2015.73.

14. von Minckwitz, G., Huang, C.S., Mano, M.S., Loibl, S., Mamounas, E.P., Untch, M., Wolmark, N., Rastogi, P., Schneeweiss, A., Redondo, A., et al. (2019). Trastuzumab Emtansine for Residual Invasive HER2-Positive Breast Cancer. N. Engl. J. Med. *380*, 617–628. https://doi.org/10.1056/NEJMoa1814017.

15. Masuda, N., Lee, S.J., Ohtani, S., Im, Y.H., Lee, E.S., Yokota, I., Kuroi, K., Im, S.A., Park, B.W., Kim, S.B., et al. (2017). Adjuvant Capecitabine for Breast Cancer after Preoperative Chemotherapy. N. Engl. J. Med. *376*, 2147–2159. https://doi.org/10.1056/NEJMoa1612645.

16. von Minckwitz, G., Blohmer, J.U., Costa, S.D., Denkert, C., Eidtmann, H., Eiermann, W., Gerber, B., Hanusch, C., Hilfrich, J., Huober, J., et al. (2013). Response-guided neoadjuvant chemotherapy for breast cancer. J. Clin. Oncol. *31*, 3623–3630. https://doi.org/10.1200/JCO.2012.45.0940.

17. Cortazar, P., Zhang, L., Untch, M., Mehta, K., Costantino, J.P., Wolmark, N., Bonnefoi, H., Cameron, D., Gianni, L., Valagussa, P., et al. (2014). Pathological complete response and long-term clinical benefit in breast cancer: the CTNeoBC pooled analysis. Lancet *384*, 164–172. https://doi.org/10.1016/S0140-6736(13)62422-8.

18. Yau, C., Osdoit, M., van der Noordaa, M., Shad, S., Wei, J., de Croze, D., Hamy, A.S., Laé, M., Reyal, F., Sonke, G.S., et al. (2022). Residual cancer burden after neoadjuvant chemotherapy and long-term survival outcomes in breast cancer: a multicentre pooled analysis of 5161 patients. Lancet Oncol. *23*, 149–160. https://doi.org/10.1016/S1470-2045(21)00589-1.

19. Cardoso, F., McArthur, H.L., Schmid, P., Cortés, J., Harbeck, N., Telli, M.L., Cescon, D.W., O'Shaughnessy, J., Fasching, P., Shao, Z., et al. (2023). KEYNOTE-756: Phase III study of neoadjuvant pembrolizumab (pembro) or placebo (pbo) + chemotherapy (chemo), followed by adjuvant pembro or pbo + endocrine therapy (ET) for early-stage high-risk ER+/Her2- breast cancer. LBA 21, ESMO congress 2023. Ann. Oncol. *34*, S1260–S1261. https://doi.org/10.1016/j.annonc.2023.10.011.

20. Loi, S., Curigliano, G., Salgado, R.F., Romero Diaz, R.I., Delaloge, S., Rojas, C., Kok, M., Saura Manich, S., Harbeck, N., Mittendorf, E.A., et al. (2023). A randomized, double-blind trial of nivolumab (NIVO) vs placebo (PBO) with neoadjuvant chemotherapy (NACT) followed by adjuvant endocrine therapy (ET) ± NIVO in patients (pts) with high-risk, ER+ HER2L primary breast cancer (BC) LBA 20, ESMO congress 2023. Ann. Oncol. *34*, S2–S2023. https://doi.org/10.1016/j.annonc.2023.10.010.

21. Parker, J.S., Mullins, M., Cheang, M.C.U., Leung, S., Voduc, D., Vickery, T., Davies, S., Fauron, C., He, X., Hu, Z., et al. (2009). Supervised risk predictor of breast cancer based on intrinsic subtypes. J. Clin. Oncol. *27*, 1160–1167. https://doi.org/10.1200/JCO.2008.18.1370.

22. Paquet, E.R., and Hallett, M.T. (2015). Absolute assignment of breast cancer intrinsic molecular subtype. J. Natl. Cancer Inst. *107*, 357.

23. Nielsen, T.O., Leung, S.C.Y., Rimm, D.L., Dodson, A., Acs, B., Badve, S., Denkert, C., Ellis, M.J., Fineberg, S., Flowers, M., et al. (2021). Assessment of Ki67 in Breast Cancer: Updated recommendations from the international Ki67 in breast cancer working group. J. Natl. Cancer Inst. *113*, 808–819. https://doi.org/10.1093/jnci/djaa201.

24. Smith, I., Robertson, J., Kilburn, L., Wilcox, M., Evans, A., Holcombe, C., Horgan, K., Kirwan, C., Mallon, E., Sibbering, M., et al. (2020). Long-term outcome and prognostic value of Ki67 after perioperative endocrine therapy in postmenopausal women with hormone-sensitive early breast cancer (POETIC): an open-label, multicentre, parallel-group, randomised, phase 3 trial. Lancet Oncol. *21*, 1443–1454. https://doi.org/10.1016/S1470-2045(20)30458-7.

25. Nitz, U.A., Gluz, O., Kümmel, S., Christgen, M., Braun, M., Aktas, B., Lüdtke-Heckenkamp, K., Forstbauer, H., Grischke, E.M., Schumacher, C., et al. (2022). Endocrine Therapy Response and 21-Gene Expression Assay for Therapy Guidance in HR+/HER2- Early Breast Cancer. J. Clin. Oncol. *40*, 2557–2567. https://doi.org/10.1200/JCO.21.02759.

26. Loibl, S., Marmé, F., Martin, M., Untch, M., Bonnefoi, H., Kim, S.B., Bear, H., McCarthy, N., Melé Olivé, M., Gelmon, K., et al. (2021). Palbociclib for Residual High-Risk Invasive HR-Positive and HER2-Negative Early Breast Cancer-The Penelope-B Trial. J. Clin. Oncol. *39*, 1518–1530. https://doi.org/10.1200/JCO.20.03639.

27. Marmé, F., Lederer, B., Blohmer, J.U., Costa, S.D., Denkert, C., Eidtmann, H., Gerber, B., Hanusch, C., Hilfrich, J., Huober, J., et al. (2016). Utility of the CPS+EG staging system in hormone receptor-positive, human epidermal growth factor receptor 2-negative breast cancer treated with neoadjuvant chemotherapy. Eur. J. Cancer *53*, 65–74. https://doi.org/10.1016/j.ejca.2015.09.022.

28. Mittendorf, E.A., Jeruss, J.S., Tucker, S.L., Kolli, A., Newman, L.A., Gonzalez-Angulo, A.M., Buchholz, T.A., Sahin, A.A., Cormier, J.N., Buzdar, A.U., et al. (2011). Validation of a novel staging system for disease-specific survival in patients with breast cancer treated with neoadjuvant chemotherapy. J. Clin. Oncol. *29*, 1956–1962. https://doi.org/10.1200/JCO.2010.31.8469.

29. Michel, L.L., Sommer, L., González Silos, R., Lorenzo Bermejo, J., von Au, A., Seitz, J., Hennigs, A., Smetanay, K., Golatta, M., Heil, J., et al. (2019). Locoregional risk assessment after neoadjuvant chemotherapy in patients with primary breast cancer: clinical utility of the CPS + EG score. Breast Cancer Res. Treat. *177*, 437–446. https://doi.org/10.1007/s10549-019-05314-9.

30. Paik, S., Shak, S., Tang, G., Kim, C., Baker, J., Cronin, M., Baehner, F.L., Walker, M.G., Watson, D., Park, T., et al. (2004). A multigene assay to predict recurrence of tamoxifen-treated, node-negative breast cancer. N. Engl. J. Med. *351*, 2817–2826. https://doi.org/10.1056/NEJMoa041588.

31. Sotiriou, C., Wirapati, P., Loi, S., Harris, A., Fox, S., Smeds, J., Nordgren, H., Farmer, P., Praz, V., Haibe-Kains, B., et al. (2006). Gene expression profiling in breast cancer: understanding the molecular basis of histologic grade to improve prognosis. J. Natl. Cancer Inst. *98*, 262–272. https://doi.org/10.1093/jnci/djj052.

32. Symmans, W.F., Hatzis, C., Sotiriou, C., Andre, F., Peintinger, F., Regitnig, P., Daxenbichler, G., Desmedt, C., Domont, J., Marth, C., et al. (2010). Genomic index of sensitivity to endocrine therapy for breast cancer. J. Clin. Oncol. *28*, 4111–4119. https://doi.org/10.1200/JCO.2010.28.4273.

33. Becht, E., McInnes, L., Healy, J., Dutertre, C.A., Kwok, I.W.H., Ng, L.G., Ginhoux, F., and Newell, E.W. (2018). Dimensionality reduction for visualizing single-cell data using UMAP. Nat. Biotechnol. *37*, 38–44. https://doi.org/10.1038/nbt.4314.

34. Yang, Y., Sun, H., Zhang, Y., Zhang, T., Gong, J., Wei, Y., Duan, Y.G., Shu, M., Yang, Y., Wu, D., and Yu, D. (2021). Dimensionality reduction by UMAP reinforces sample heterogeneity analysis in bulk transcriptomic data. Cell Rep. *36*, 109442. https://doi.org/10.1016/j.celrep.2021.109442.

35. Staaf, J., Häkkinen, J., Hegardt, C., Saal, L.H., Kimbung, S., Hedenfalk, I., Lien, T., Sørlie, T., Naume, B., Russnes, H., et al. (2022). RNA sequencing-based single sample predictors of molecular subtype and risk of recurrence for clinical assessment of early-stage breast cancer. NPJ Breast Cancer *8*, 94. https://doi.org/10.1038/s41523-022-00465-3.

36. Prat, A., Ellis, M.J., and Perou, C.M. (2011). Practical implications of gene-expression-based assays for breast oncologists. Nat. Rev. Clin. Oncol. *9*, 48–57. https://doi.org/10.1038/nrclinonc.2011.178.

37. Bedard, P.L., Hansen, A.R., Ratain, M.J., and Siu, L.L. (2013). Tumour heterogeneity in the clinic. Nature *501*, 355–364. https://doi.org/10.1038/nature12627.

38. Kurtz, D.M., Esfahani, M.S., Scherer, F., Soo, J., Jin, M.C., Liu, C.L., Newman, A.M., Dührsen, U., Hüttmann, A., Casasnovas, O., et al. (2019). Dynamic Risk Profiling Using Serial Tumor Biomarkers for Personalized Outcome Prediction. Cell *178*, 699–713.e19. https://doi.org/10.1016/j.cell.2019.06.011.

39. Foukakis, T., Lövrot, J., Sandqvist, P., Xie, H., Lindström, L.S., Giorgetti, C., Jacobsson, H., Hedayati, E., and Bergh, J. (2015). Gene expression profiling of sequential metastatic biopsies for biomarker discovery in breast cancer. Mol. Oncol. *9*, 1384–1391. https://doi.org/10.1016/j.molonc.2015.03.011.

40. Hancock, B.A., Chen, Y.H., Solzak, J.P., Ahmad, M.N., Wedge, D.C., Brinza, D., Scafe, C., Veitch, J., Gottimukkala, R., Short, W., et al. (2019). Profiling molecular regulators of recurrence in chemorefractory triple-negative breast cancers. Breast Cancer Res. *21*, 87. https://doi.org/10.1186/s13058-019-1171-7.

41. Chen, P.L., Roh, W., Reuben, A., Cooper, Z.A., Spencer, C.N., Prieto, P.A., Miller, J.P., Bassett, R.L., Gopalakrishnan, V., Wani, K., et al. (2016). Analysis of Immune Signatures in Longitudinal Tumor Samples Yields Insight into Biomarkers of Response and Mechanisms of Resistance to Immune Checkpoint Blockade. Cancer Discov. *6*, 827–837. https://doi.org/10.1158/2159-8290.CD-15-1545.

42. Seo, S., Ryu, M.H., Park, Y.S., Ahn, J.Y., Park, Y., Park, S.R., Ryoo, B.Y., Lee, G.H., Jung, H.Y., and Kang, Y.K. (2019). Loss of HER2 positivity after anti-HER2 chemotherapy in HER2-positive gastric cancer patients: results of the GASTric cancer HER2 reassessment study 3 (GASTHER3). Gastric Cancer *22*, 527–535. https://doi.org/10.1007/s10120-018-0891-1.

43. Powles, T., Kockx, M., Rodriguez-Vida, A., Duran, I., Crabb, S.J., Van Der Heijden, M.S., Szabados, B., Pous, A.F., Gravis, G., Herranz, U.A., et al. (2019). Clinical efficacy and biomarker analysis of neoadjuvant atezolizumab in operable urothelial carcinoma in the ABACUS trial. Nat. Med. *25*, 1706–1714. https://doi.org/10.1038/s41591-019-0628-7.

44. Keam, S.P., Halse, H., Nguyen, T., Wang, M., Van Kooten Losio, N., Mitchell, C., Caramia, F., Byrne, D.J., Haupt, S., Ryland, G., et al. (2020). High dose-rate brachytherapy of localized prostate cancer converts tumors from cold to hot. J. Immunother. Cancer *8*, e000792. https://doi.org/10.1136/jitc-2020-000792.

45. Dowsett, M., Ebbs, S.R., Dixon, J.M., Skene, A., Griffith, C., Boeddinghaus, I., Salter, J., Detre, S., Hills, M., Ashley, S., et al. (2005). Biomarker changes during neoadjuvant anastrozole, tamoxifen, or the combination: influence of hormonal status and HER-2 in breast cancer–a study from the IMPACT trialists. J. Clin. Oncol. *23*, 2477–2492. https://doi.org/10.1200/JCO.2005.07.559.

46. Miller, W.R., Larionov, A.A., Renshaw, L., Anderson, T.J., White, S., Murray, J., Murray, E., Hampton, G., Walker, J.R., Ho, S., et al. (2007). Changes in breast cancer transcriptional profiles after treatment with the aromatase inhibitor, letrozole. Pharmacogenetics Genom. *17*, 813–826. https://doi.org/10.1097/FPC.0b013e32820b853a.

47. Miller, W.R., Larionov, A., Renshaw, L., Anderson, T.J., Walker, J.R., Krause, A., Sing, T., Evans, D.B., and Dixon, J.M. (2009). Gene expression profiles differentiating between breast cancers clinically responsive or resistant to letrozole. J. Clin. Oncol. *27*, 1382–1387. https://doi.org/10.1200/JCO.2008.16.8849.

48. Dowsett, M., Smith, I., Robertson, J., Robison, L., Pinhel, I., Johnson, L., Salter, J., Dunbier, A., Anderson, H., Ghazoui, Z., et al. (2011). Endocrine therapy, new biologicals, and new study designs for presurgical studies in breast cancer. J. Natl. Cancer Inst. Monogr. *2011*, 120–123. https://doi.org/10.1093/jncimonographs/lgr034.

49. Magbanua, M.J.M., Wolf, D.M., Yau, C., Davis, S.E., Crothers, J., Au, A., Haqq, C.M., Livasy, C., Rugo, H.S.; I-SPY 1 TRIAL Investigators, and Esserman, L. (2015). Serial expression analysis of breast tumors during neoadjuvant chemotherapy reveals changes in cell cycle and immune pathways associated with recurrence and response. Breast Cancer Research *17*, 1–13. https://doi.org/10.1186/s13058-015-0582-3.

50. Nitz, U., Gluz, O., Kreipe, H.H., Christgen, M., Kuemmel, S., Baehner, F.L., Shak, S., Aktas, B., Braun, M., Lüdtke-Heckenkamp, K., et al. (2020). The run-in phase of the prospective WSG-ADAPT HR+/HER2- trial demonstrates the feasibility of a study design combining static and dynamic biomarker assessments for individualized therapy in early breast cancer. Ther. Adv. Med. Oncol. *12*, 1758835920973130. https://doi.org/10.1177/1758835920973130.

51. Yates, L.R., Gerstung, M., Knappskog, S., Desmedt, C., Gundem, G., Van Loo, P., Aas, T., Alexandrov, L.B., Larsimont, D., Davies, H., et al. (2015). Subclonal diversification of primary BC revealed by multiregion sequencing. Nat. Med. *21*, 751–759. https://doi.org/10.1038/nm.3886.

52. Turner, N.C., Ro, J., André, F., Loi, S., Verma, S., Iwata, H., Harbeck, N., Loibl, S., Huang Bartlett, C., Zhang, K., et al. (2015). Palbociclib in Hormone-Receptor-Positive Advanced Breast Cancer. N. Engl. J. Med. *373*, 209–219. https://doi.org/10.1056/NEJMoa1505270.

53. Mayer, E.L., Dueck, A.C., Martin, M., Rubovszky, G., Burstein, H.J., Bellet-Ezquerra, M., Miller, K.D., Zdenkowski, N., Winer, E.P., Pfeiler, G., et al. (2021). Palbociclib with adjuvant endocrine therapy in early breast cancer (PALLAS): interim analysis of a multicentre, open-label, randomised, phase 3 study. Lancet Oncol. *22*, 212–222. https://doi.org/10.1016/S1470-2045(20)30642-2.

54. Gnant, M., Dueck, A.C., Frantal, S., Martin, M., Burstein, H.J., Greil, R., Fox, P., Wolff, A.C., Chan, A., Winer, E.P., et al. (2022). Adjuvant Palbociclib for Early Breast Cancer: The PALLAS Trial Results (ABCSG-42/AFT-05/BIG-14-03). J. Clin. Oncol. *40*, 282–293. https://doi.org/10.1200/JCO.21.02554.

55. Weigelt, B., Hu, Z., He, X., Livasy, C., Carey, L.A., Ewend, M.G., Glas, A.M., Perou, C.M., and Van't Veer, L.J. (2005). Molecular portraits and 70-gene prognosis signature are preserved throughout the metastatic process of breast cancer. Cancer Res. *65*, 9155–9158. https://doi.org/10.1158/0008-5472.CAN-05-2553.

56. Shinmura, K., and Yokota, J. (2001). The OGG1 gene encodes a repair enzyme for oxidatively damaged DNA and is involved in human carcinogenesis. Antioxidants Redox Signal. *3*, 597–609. https://doi.org/10.1089/15230860152542952.

57. Whitmore, A., Freeny, D., Sojourner, S.J., Miles, J.S., Graham, W.M., and Flores-Rozas, H. (2020). Evaluation of the Role of Human DNAJAs in the Response to Cytotoxic Chemotherapeutic Agents in a Yeast Model System. BioMed Res. Int. *2020*, 9097638. https://doi.org/10.1155/2020/9097638.

58. He, C.H., and Ramotar, D. (1999). An allele of the yeast RPB7 gene, encoding an essential subunit of RNA polymerase II, reduces cellular resistance to the antitumor drug bleomycin. Biochem. Cell. Biol. *77*, 375–382.

59. Timson, D.J., Singleton, M.R., and Wigley, D.B. (2000). DNA ligases in the repair and replication of DNA. Mutat. Res. *460*, 301–318. https://doi.org/10.1016/s0921-8777(00)00033-1.

60. Puts, G.S., Leonard, M.K., Pamidimukkala, N.V., Snyder, D.E., and Kaetzel, D.M. (2018). Nuclear functions of NME proteins. Lab. Invest. *98*, 211–218. https://doi.org/10.1038/labinvest.2017.109.

61. Limpose, K.L., Trego, K.S., Li, Z., Leung, S.W., Sarker, A.H., Shah, J.A., Ramalingam, S.S., Werner, E.M., Dynan, W.S., Cooper, P.K., et al. (2018). Overexpression of the base excision repair NTHL1 glycosylase causes genomic instability and early cellular hallmarks of cancer. Nucleic Acids Res. *46*, 4515–4532. https://doi.org/10.1093/nar/gky162.

62. Vila, J., Teshome, M., Tucker, S.L., Woodward, W.A., Chavez-MacGregor, M., Hunt, K.K., and Mittendorf, E.A. (2017). Combining Clinical and Pathologic Staging Variables Has Prognostic Value in Predicting Local-regional Recurrence Following Neoadjuvant Chemotherapy for Breast Cancer. Ann. Surg. *265*, 574–580. https://doi.org/10.1097/SLA.0000000000001492.

63. Gao, Q., López-Knowles, E., U Cheang, M.C., Morden, J., Ribas, R., Sidhu, K., Evans, D., Martins, V., Dodson, A., Skene, A., et al. (2018). Major Impact of Sampling Methodology on Gene Expression in Estrogen Receptor- Positive Breast Cancer. JNCI Cancer Spectr. *2*, pky005. https://doi.org/10.1093/jncics/pky005.

64. Haibe-Kains, B., and Cescon, D.W. (2018). Gene Expression Analyses in Breast Cancer: Sample Matters. JNCI Cancer Spectr. *2*, pky019. https://doi.org/10.1093/jncics/pky019.

65. Finn, R.S., Martin, M., Rugo, H.S., Jones, S., Im, S.A., Gelmon, K., Harbeck, N., Lipatov, O.N., Walshe, J.M., Moulder, S., et al. (2016). Palbociclib and Letrozole in Advanced Breast Cancer. N. Engl. J. Med. *375*, 1925–1936. https://doi.org/10.1056/NEJMoa1607303.

66. Brueffer, C., Gladchuk, S., Winter, C., Vallon-Christersson, J., Hegardt, C., Häkkinen, J., George, A.M., Chen, Y., Ehinger, A., Larsson, C., et al. (2020). The mutational landscape of the SCAN-B real-world primary breast cancer transcriptome. EMBO Mol. Med. *12*, e12118. https://doi.org/10.15252/emmm.202012118.

67. Gendoo, D.M.A., Ratanasirigulchai, N., Schröder, M.S., Paré, L., Parker, J.S., Prat, A., and Haibe-Kains, B. (2016). Genefu: an R/Bioconductor package for computation of gene expression-based signatures in breast cancer. Bioinformatics *32*, 1097–1099. https://doi.org/10.1093/bioinformatics/btv693.

68. Sinn, B.V., Fu, C., Lau, R., Litton, J., Tsai, T.H., Murthy, R., Tam, A., Andreopoulou, E., Gong, Y., Murthy, R., et al. (2019). SET ER/PR: a robust 18-gene predictor for sensitivity to endocrine therapy for metastatic breast cancer. NPJ Breast Cancer *5*, 16. https://doi.org/10.1038/s41523-019-0111-0.

69. Vallon-Christersson, J. (2023). RNA Sequencing-Based Single Sample Predictors of Molecular Subtype and Risk of Recurrence for Clinical Assessment of Early-Stage Breast Cancer. Mendeley Data *V3*. https://doi.org/10.17632/yzxtxn4nmd.3.

70. Cancer Genome Atlas Network (2012). Comprehensive molecular portraits of human breast tumours. Nature *490*, 61–70. https://doi.org/10.1038/nature11412.

71. Subramanian, A., Tamayo, P., Mootha, V.K., Mukherjee, S., Ebert, B.L., Gillette, M.A., Paulovich, A., Pomeroy, S.L., Golub, T.R., Lander, E.S., and Mesirov, J.P. (2005). Gene set enrichment analysis: a knowledge-based approach for interpreting genome-wide expression profiles. Proc. Natl. Acad. Sci. USA *102*, 15545–15550.

72. Liberzon, A., Subramanian, A., Pinchback, R., Thorvaldsdóttir, H., Tamayo, P., and Mesirov, J.P. (2011). Molecular signatures database (MSigDB) 3.0. Bioinformatics *27*, 1739–1740.

STAR★METHODS

KEY RESOURCES TABLE

REAGENT or RESOURCE	SOURCE	IDENTIFIER
Biological samples		
Tumor biopsies and data from the Penelope clinical trial	Loibl et al.[26]	NCT01864746; EudraCT 2013-001040-62
Data generated from tumor biopsies from the Sweden Cancerome Analysis Network-Breast (SCAN-B;) population-based cohort (NCT02306096)	Vallon-Christersson J.[69]	https://data.mendeley.com/datasets/yzxtxn4nmd/3
Gene expression data generated as part of the TCGA consortium for validation of AIMS algorithm	Cancer Genome Atlas Network[70]	https://gdac.broadinstitute.org/runs/stddata__2016_01_28/data/BRCA/20160128/gdac.broadinstitute.org_BRCA.Merge_rnaseqv2__illuminahiseq_rnaseqv2__unc_edu__Level_3__RSEM_genes__data.Level_3.2016012800.0.0.tar.gz
Critical commercial assays		
Oncology Biomarker mRNA Panel, ILM Kit, 1x96	HTG Molecular Diagnostics, Tucson, Arizona, US	916-002-096
Deposited data		
Data for this study	GitHub	https://github.com/tkarn/Penelope-HTG
R script with analysis code	GitHub	https://github.com/tkarn/Penelope-HTG
Output files	GitHub	https://github.com/tkarn/Penelope-HTG
Data, output and analysis code	Zenodo	https://doi.org/10.5281/zenodo.14192594
Software and algorithms		
R version 4.2.1	The R Project for Statistical Computing	https://www.r-project.org
Package for AIMS	R/Bioconductor	https://bioconductor.org/packages/release/bioc/html/AIMS.html
ggsankey package (v 0.0.99999)	GitHub	https://github.com/davidsjoberg/ggsankey
LIMMA (v3.50.3) in R for analysis of differential gene expression	R/Bioconductor	https://bioconductor.org/packages/release/bioc/html/limma.html
ComplexHeatmap package (v2.13.1)	R/Bioconductor	https://bioconductor.org/packages/release/bioc/html/ComplexHeatmap.html
GSEA software, version 4.2.3	Subramanian et al.[71]	https://www.gsea-msigdb.org/gsea/index.jspMSigDB
The Molecular Signatures Database (MSigDB	Liberzon et al.[72]	https://www.gsea-msigdb.org/gsea/msigdb
Statistical analysis software	SAS version 9.4	(SAS Institute Inc., Cary, NC)

EXPERIMENTAL MODEL AND STUDY PARTICIPANT DETAILS

Study design and clinical cohorts

The Penelope-B trial (NCT01864746; EudraCT 2013-001040-62) is a prospective, multicenter, multinational, randomized, double-blind, placebo-controlled phase 3 clinical trial in patients with hormone-receptor positive breast cancer without complete response to taxane-containing neoadjuvant chemotherapy with high-risk residual disease.[26] An overview on the complete study setup is shown in Figure 1. The aim of the trial was to investigate the addition of the CDK4/6 inhibitor Palbociclib after the neoadjuvant therapy for one year to standard adjuvant endocrine therapy. High-risk residual disease was predefined based on CPS-EG score, a combination of the pre-treatment clinical stage and post-treatment pathologic stage (CPS) as well as estrogen receptor status (E) and tumor grade (G). Tumors with a CPS-EG score ≥ 3 or with a score of 2 and ypN1-stage were defined as high-risk residual disease. Patients must have received NACT for at least 16 weeks (including 6 weeks of a taxane) followed by definitive surgery (including resection of all clinically evident invasive disease and ipsilateral axillary lymph node dissection or sentinel node biopsy) and radiation as indicated according to local guidelines. Further details of patient recruitment have been published.[26]

After the completion of neoadjuvant therapy, patients were randomly assigned (1:1) to receive 13 cycles of Palbociclib 125 mg once daily or placebo on days 1-21 in a 28-day cycle in addition to endocrine therapy (ET) for a total duration of 1 year (corresponding to 13 4-week cycles). Standard adjuvant ET was given at the discretion of the investigator for at least 5 years.

Primary end point is invasive disease-free survival (iDFS). The Penelope-B trial was sponsored by GBG Forschungs GmbH in collaboration with NSABP Foundation (plus I-SPY and CCTR), ABCSG, AGO-B, ANBCSG, BIG, Geicam, ICR-CTSU, JBCSG, and KCSG. Pfizer Inc funded the trial and provided drug. The trial was conducted according to ICH-GCP guidelines and the Declaration of Helsinki. All patients provided written informed consent for trial participation, data transfer, and biomaterial collection. The translational investigations were approved by the Ethics Committee of the Philipps-University Marburg (Project 38/20).

As validation cohort, the Sweden Cancerome Analysis Network-Breast (SCAN-B; NCT02306096) population-based cohort was used.[35,66]

METHOD DETAILS

Endpoints

The primary endpoint was invasive disease-free survival (iDFS), defined as the time between randomization and the first event (ipsilateral invasive in-breast or locoregional recurrence, distant recurrence, invasive contralateral breast cancer, second primary invasive cancer [nonbreast], or death because of any cause).

Biobanking and central pathology

Central histopathological assessment of formalin-fixed paraffin-embedded tumor biopsies was required before randomization, preferably on post-neoadjuvant residual invasive disease of the breast, or if not possible, of residual nodal invasion or core biopsy. Expression of estrogen receptors, progesterone receptors, HER2 and Ki-67 was evaluated by immunohistochemistry. Estrogene (ER) and progesterone receptor (PR) positivity were defined as $\geq$1% stained cells, and HER2 negativity as immunohistochemistry score 0-1 or HER2 in-situ hybridization test ratio <2.0. The tumor samples, including residual tumor after NACT as well as core biopsies before NACT were stored in a central biobank for translational research projects, including gene-expression profiling.

Gene expression analysis in pre-therapeutic and post-therapeutic samples

Gene expression in pre-Tx (n=629) biopsies and post-Tx (n=782) surgical resections and metastatic (n=43) FFPE tumor tissues was profiled using the HTG EdgeSeq Oncology Biomarker Panel (HTG OBP) that measures expression of 2549 genes associated with tumor biology (https://www.htgmolecular.com/assays/obp/genes). Paired gene expression data (pre-Tx and post-Tx) from the same patient was available for 540 tumors. Similarly, 29 tumors had gene expression data for all the three tissues (pre-Tx biopsy, post-Tx resections and metastatic disease).

For quality control of HTG measurements, the mean of four negative and four positive internal controls was calculated for each sample. The measurement was repeated for a sample if the mean of its positive controls was below two standard deviations (SDs) of the grand mean across all samples or if the mean of its negative controls was above two SDs from the grand mean. As an additional quality control, samples with less than 1.5 million total counts were excluded from further analysis. The quality-controlled data was normalized using the counts per million (CPM) method and log2-transformation. Finally, to improve reproducibility a modification of the CPM method was applied by introducing a lower bound of 3. The normalized log2-transformed values were used for all the analyses involving HTG genes except for the AIMS subtype.

Molecular analyses – AIMS subtypes

Absolute Intrinsic Molecular Subtyping (AIMS) algorithm was used to assign the molecular subtypes in the Penelope-B cohort. Gene expression data on 91 of the 151 genes processed by AIMS are available in the HTG assay. To assess the accuracy of the AIMS method based on this reduced number of genes, we have evaluated the original AIMS method as well as the adaptation to 91 genes in the TCGA cohort. The concordance of the AIMS subtypes are shown in Tables S2 and S3 for the complete TCGA cohort and the HRpositive/HER2negative samples, respectively. Detailed analysis code and output is available on GitHub resource.

Based on these 91 genes, the AIMS subtype was calculated individually for pre-Tx, post-Tx and metastatic tumors from the HTG count data. Sankey plots were generated using ggsankey package (v 0.0.99999) for AIMS data for pre-Tx, post-Tx and metastatic tumors as well as AC-subtypes.

Differential gene expression analysis, clustering and UMAP analysis

The normalized counts for pre- and post-Tx in paired samples were analysed for differential gene expression using LIMMA (v3.50.3) in R, and volcano plots were drawn for genes that were statistically significant for FDR adjusted p-value < 0.05.

Briefly, for differential gene expression analysis the pre- and post-Tx data was quantile normalized followed by estimation of the correlation between duplicate or repeated samples using duplicateCorrelation function. This correlation was incorporated into the linear model fitting process using the lmFit function. Contrast matrices were then applied to define the comparisons of interest, and the data were analyzed to identify differentially expressed genes. The eBayes function was used to compute moderated t-statistics, log-odds, and adjusted p-values. All analyses were performed using default parameters unless otherwise specified.

Among the differentially expressed genes between biopsy and surgical samples 15 were known to be highly inducible by pre-analytical factors.[63,64] These 15 genes were removed from the volcano plot in Figure 2 for clarity but were included in Figure S2 as well as in the clustering and the UMAP analysis. The reason was not to alter the primary dataset by removal of a small number of genes, which might result in bias and overfitting and lead to problems in follow-up studies. Furthermore, the degree of association between individual genes and pre-analytical factors is a continuous parameter and no clear cutoff is available to decide how many genes should be excluded. In the subsequent cluster analysis (see below), all 15 genes are in gene cluster-4, and 9 of these 15 genes showed statistically significantly improved iDFS. Therefore, our strategy was to state clearly that these genes are regulated by factors related to cellular stress during surgery, but to leave these genes in the analysis dataset.

Unsupervised hierarchical clustering was performed on genes with a differential expression of ±0.58 log2FC (1.5-fold change) using Euclidean distance and the ward.D2 method via the ComplexHeatmap package in R. Additionally, K-means clustering was applied at specific levels of the dendrogram to identify clusters of similar data points for both genes and samples. To ensure robust clustering results, km_repeats were set to 100, repeating the K-means clustering process multiple times. The choice of 4 row clusters and 10 sample clusters (eventually clustering showed 9) was based on the expected number of distinct groups or patterns in AIMS subtypes pre- and post-Tx.

In addition, UMAP was generated with euclidean metric for the same set of 335 genes from the hierarchical clustering heatmap. A ggplot visualization was created in R, with points colored by Adaptive clusters or pre.AIMS subtypes and shaped by pre.Tx or post.Tx.

Definition of gene groups for analysis of prognostic markers

Gene clustering was derived from the heatmap based on the cluster analysis of the paired samples. From this analysis, four main gene clusters were derived, cluster-1 was analyzed in more detail with a focus on the four subclusters 1A to 1D. The main characteristics of each gene cluster was used for labelling and color coding.

For some prognostic analyses, the samples were grouped into tertiles based on the mean expression of all genes in the cluster, it should be recognized that these tertiles might not reflect the optimal cutpoint for each gene cluster.

For comparison of the gene clusters with TCGA samples, RNA-Seq data for 1215 BRCA samples from TCGA were downloaded from UCSC cancer browser (https://genome-cancer.ucsc.edu/); dataset ID TCGA_BRCA_exp_HiSeqV2, version "2015-01-28"). This dataset contains 1095 primary tumors, 7 metastasis, 113 normal tissue samples. Median centered gene expression data of the 335 differentially expressed genes (DEG) from the Penelope analysis were used for hierarchical clustering of TCGA samples.

Evaluation of prognostic markers in pre-Tx and post-Tx samples

For comparison of genes relevant for prognosis in either pre-Tx biopsies or post-Tx tumor resections all 335 differentially regulated genes were displayed in a scatter plot according to their impact on disease free survival in either pre-Tx biopsies (x-axis) or post-Tx resections (y-axis). The inverse hazard ratio (1/HR) was shown, so that genes that are linked to improved survival in both pre-Tx and post-Tx tumors are located in the upper right quadrant, and colored according to the gene clusters and their functional annotation (detailed code available on GitHub resource).

Gene set enrichment analysis

Gene Set Enrichment Analysis (GSEA) determines whether *a priori* defined set of genes shows statistically significant, concordant differences between two phenotypes. For GSEA, the 2549 genes of the HTG OBP panel were mapped to 25 gene groups and pathways predefined by HTG (HTG gene sets), as well as to the established 50 hallmark (HM) gene sets of the Human Molecular Signatures Database (v2023.2) representing well-defined biological states and processes. GSEA was performed on 540 paired pre- and post-Tx samples using two methods: phenotype-based and pre-ranked. For the phenotype-based method, normalized expression data for 2,549 genes across 1,080 samples was analyzed. The analysis utilized 2,500 permutations, a weighted enrichment statistic, and the Signal2Noise metric, with all other parameters set to default. For the pre-ranked method, GSEA was conducted using the regression parameters derived from univariate Cox regression analysis for both pre- and post-Tx conditions. This analysis employed the GSEAPreranked tool, using a rank metric based on the p-values and the sign of the test statistic from regression analyses, calculated as -log10(p-value) * sign(test statistic). Positive values of the rank metric indicate genesets more likely to be upregulated in patients with longer survival, while negative values indicate the opposite.The key metrics of GSEA enriched score and normalized enrichment scores were scored using default conditions with few modifications (max size to exclude larger sets=750, min size to exclude smaller sets=10) to include all the gene sets for the analysis. The threshold for significant enrichment were defined as a p-value of <0.05 and an FDR of <0.25. The statistically significant gene sets were displayed as dot plots generated in R. The GSEA was carried out using Microsoft Windows-based software v.4.3.2.

Generation of centroids

The sample groups identified by K-means clustering were designated as Adaptive clusters (AC-1 to AC-9). For each of the Adaptive cluster, centroids were calculated, representing the mean position of all the points within a cluster and serving as a reference for cluster characterization. Finally, sample clusters and corresponding data were extracted, and the data was scaled columnwise and centered before calculating the centroids.

The centroids obtained from the clustering process were then used to classify test samples. This involved, scaling and centering the data, measuring the distance of each sample to the cluster centroids and assigning the sample to the nearest cluster. This step ensured that the clustering model was robust and generalizable to new, unseen data.

Evaluation of the existing gene signatures recurrence score, GGI, SET index

Signature scores for "Recurrence Score" (RS), "Genomic Grade Index" (GGI), and "Sensitivity to Endocrine Therapy Index" (SET), were calculated for 812 ER positive breast cancer samples from TCGA, by using either all genes from the signatures or only the subset of genes available in the HTG oncobiology panel. Scatter plots show the correlation (Pearson R value) and the distribution of the respective signature scores. Calculation of RS[30] and GGI[31] were adapted from genefu package,[67] and SET[32] from Sinn 2019.[68] Detailed code is provided in the online resources on GitHub.

Evaluation of SCAN-B cohort

For validation of our AC classification model, we obtained RNA-seq data and corresponding clinical data for the SCAN-B cohort, the link is given in the key resource table. A total of 3764 patients diagnosed with hormone receptor positive, HER2 negative, primary invasive breast cancer were included in the present analysis. These comprise 57% of the 6660-sample early-stage follow-up cohort (one patient – one tumor RNA sequencing profile) from the total set of 9206 RNA sequencing profiles. The gene expression data for the 335 genes identified from Penelope analysis was extracted and log2 transformed with an offset of 0.1 before scaled and centered. Finally, the data was cluster classified using the centroid algorithm developed based on the Penelope data. The resultant Adaptive clusters were cross-tabulated with NCN.PAM50 subtypes and subsequently checked for their association with Distant Recurrence-Free Interval (DRFi) using Kaplan-Meier analysis.

QUANTIFICATION AND STATISTICAL ANALYSIS

Differences between the patient groups with and without HTG gene expression data in Peneleope cohort were assessed using chi-square for categorical variables and paired- t test or Wilcoxon signed-rank test for continuous variables. All the statistical tests were performed as 2-sided at significance level $P<0.05$. The association of the clinical variables and HTG genes on iDFS was assessed using univariate Cox regression models and represented as hazard ratios (HRs) with 95% confidence intervals (95% CI). Statistical significance was assessed by using Wald tests. The patients without iDFS at the end of the follow-up time were censored. In addition, a Cox regression model with interaction term was carried out to determine an interaction of luminal types and treatment arm on iDFS. Kaplan-Meier cumulative curves for the iDFS as outcome were drawn for patients with and without treatment arm, for AIMS subtypes in pre- and post-Tx groups and for the Adaptive clusters. Differences between the groups were analyzed by the log-rank test. Similarly, survival curves based on Adaptive clusters were also drawn for SCAN-B cohort with DRFi as endpoint. All statistical analyses were carried out by using SAS version 9.4 (SAS Institute Inc., Cary, NC).